

1 **ANEMI_Yangtze v1.0: A Coupled Human-Natural Systems Model for the Yangtze**
2 **Economic Belt - Model Description**

3 Haiyan Jiang^{1,2,3*}, Slobodan P. Simonovic¹, Zhongbo Yu^{2,4,5}

4 ¹Department of Civil and Environmental Engineering, Western University, London, Ontario,
5 Canada

6 ²State Key Laboratory of Hydrology-Water Resources and Hydraulic Engineering, Hohai
7 University, Nanjing, 210098, China

8 ³College of Urban Construction, Nanjing Tech University, Nanjing, 211816, China

9 ⁴Joint International Research Laboratory of Global Change and Water Cycle, Hohai University,
10 Nanjing, 210098, China

11 ⁵Yangtze Institute for Conservation and Development, Hohai University, Nanjing, 210098, China

12 **Correspondence:** Haiyan Jiang (sophia4637@163.com; hjiang95@uwo.ca)

13 **Abstract:** Yangtze Economic Belt (hereafter Belt) is one of the most dynamic regions in China in
14 terms of population growth, economic progress, industrialization, and urbanization. It faces many
15 resource constraints (land, food, energy) and environmental challenges (pollution, biodiversity
16 loss) under rapid population growth and economic development. Interactions between human and
17 natural systems are at the heart of the challenges facing the sustainable development of the Belt.
18 By adopting the system thinking and the methodology of system dynamics simulation, an
19 integrated system dynamics-based simulation model for the Belt, named ANEMI_Yangtze, is
20 developed based on the third version of ANEMI3. Nine sectors of population, economy, land, food,
21 energy, water, carbon, nutrients, and fish are currently included in ANEMI_Yangtze.

22 This paper presents the ANEMI_Yangtze model description, which includes: (i) the identification
23 of the cross-sectoral interactions and feedbacks involved in shaping the Belt's system behaviour
24 over time; (ii) the identification of the feedbacks within each sector that drive the state variables
25 in that sector; and (iii) the description of a new *Fish Sector* and modifications in the *Population*,
26 *Food*, *Energy*, and *Water Sectors*, including the underlying theoretical basis for model equations.

27 The validation and robustness tests confirm that the ANEMI_Yangtze model can be used to
28 support scenario development, policy assessment, and decision making. This study aims to
29 improve the understanding of the complex interactions among coupled human-natural systems in
30 the Belt to provide the foundation for science-based policies for the sustainable development of
31 the Belt.

32 **Keywords:** ANEMI_Yangtze; coupled human and nature systems; system dynamics simulation;
33 Yangtze Economic Belt;

34 **1. Introduction**

35 Today global problems and challenges facing humanity are becoming more and more
36 complex and directly related to the areas of energy, water, and food production, distribution, and
37 use (Hopwood et al., 2005; Bazilian et al., 2011; Akhtar et al., 2013; van Vuuren et al., 2015;
38 D’Odorico et al., 2018). The relations linking human race to the biosphere are so complex that all
39 aspects affect each other. Knowledge and methods from a single discipline are no longer sufficient
40 to address these complex, interrelated problems that characterize as fundamental threats to human
41 society (Klein et al., 2001; Bazilian et al., 2011; Clayton and Radcliffe, 2018; Calvin and Bond-
42 Lamberty 2018). Understanding the mechanism of the dynamics within the coupled human-natural
43 systems calls for cooperation across wide-range of disciplines and knowledge domains (Liu et al.
44 2007; Fu, 2020). The combination of quantitative multi-sector modelling and scenario analysis has
45 emerged as a well-suited methodology paradigm for studying coupled human-natural systems and
46 exploring future pathways and policy implications (Hertwich et al., 2015; Allen et al., 2016; Fu,
47 2020).

48 Multi-sector modelling mainly occurs within two modelling paradigms: Integrated
49 Assessment Modelling (IAM) and System Dynamics simulation (SD). IAMs are developed and
50 used for addressing complex interactions between socio-economic and natural sectors. They
51 integrate knowledge from various disciplines into a single modelling environment and are used to
52 investigate future adaptation pathways to globally changing conditions (van Beek et al., 2020).
53 There are several IAMs of global change. Examples include AIM (Matsuoka et al., 1995),
54 MESSAGE (Messner and Strubegger, 1995; Messner and Schrattenholzer, 2000; Sullivan et al.,
55 2013), POLES (European Commission, 1996), TIMES (Loulou, 2007), REMIND (Bauer et al.,
56 2012; Kriegler et al., 2017), IMAGE (Stehfest et al., 2014), and GCAM (Calvin et al., 2019), to
57 name a few. The most often used IAMs approach is the static approach in which to connect
58 disciplinary models output of one model is first obtained then given as input to another. This
59 approach is not well suited for studying feedback relationships between different sectors.

60 The second modelling paradigm – System Dynamics simulation (SD) – integrates all sectoral
61 models into the endogenous structures with emphasis on the link between the system structure and
62 dynamic behaviour through explicit consideration of multiple feedback relations. This approach is

63 the only way to create and thoroughly study feedback relationships between different sectors
64 (Davies and Simonovic, 2010; Pedercini et al., 2019; Qu et al., 2020). There are also several SD
65 models of global change. Examples include ANEMI (Davies and Simonovic, 2010, 2011; Akhtar
66 et al., 2013, 2019; Breach and Simonovic, 2021), Threshold 21 (Qu et al, 1995; Qu et al., 2020),
67 and iSDG (Pedercini et al., 2019). ANEMI is intended for analyzing long-term (2100) global
68 feedbacks (at the global scale) with emphasis on the role of water resources. Threshold 21 and
69 iSDG are structured to analyze medium (2030) to long-term (2050) development issues at the
70 national scale.

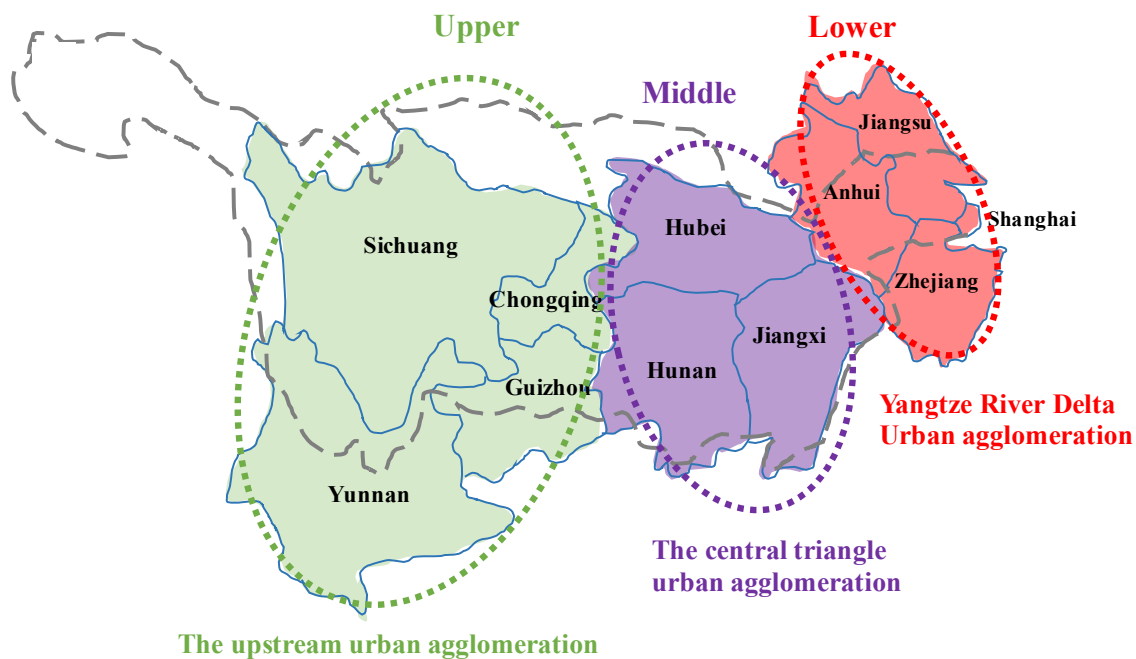
71 These IAMs and SDs provide valuable tools to assess the impacts of global change and
72 adaptation and vulnerability of human society. However, most of these models are highly
73 aggregated. This level of aggregation limits the level of detail that can be represented (Breach and
74 Simonovic, 2021). Therefore, there is an urgent need for model downscaling (Holman et al., 2008;
75 Bazilian et al., 2011; Akhtar et al., 2019; Fisher-Vanden and Weyant, 2020). For example, the
76 GCAM model currently has several sub-national versions, including GCAM-USA (Shi et al.,
77 2017), GCAM-China (Yu et al., 2020), GCAM-Korea (Jeon et al., 2020) and others in
78 development. Recently, there have even been calls for downscaling models to the city level
79 (Dermody et al., 2018). Another way of capturing regional or local processes is to develop regional
80 or local integrated models from scratch. For instance, the coupled water supply-power generation-
81 environment systems model developed for the upper Yangtze river basin in China (Jia et al., 2021).
82 However, due to the considerable complexities in the coupled human-natural systems at the local
83 scale, research aimed at addressing local-specific challenges is relatively limited, especially for
84 regions with fast socio-economic development (Wang et al., 2019).

85 Yangtze Economic Belt, one of the most dynamic regions in China in terms of population
86 growth and economic development, accounts for about 40% of the country's population and GDP
87 and 1/15 of the global population. The Belt's fast urbanization and economic prosperity come at
88 the cost of the environment (Xu et al., 2018). To repair its deteriorating eco-environment, the Belt's
89 development paradigm has shifted from "large-scale development" to "green development".
90 However, it remains poorly understood how the coupled human-natural systems in the Belt interact?
91 To enhance understanding of the complex interactions among human and natural systems in the
92 Belt and to provide the foundation for science-based policy-making for the sustainable
93 development of the Belt, we developed the ANEMI_Yangtze model. This paper focuses on model

94 description and would be an important addition to the literature. The model application, which
 95 helps us understand how the Belt will evolve under a particular set of conditions and how the
 96 system will change in response to a wide range of policy scenarios, is available in Jiang et al.
 97 (2021). The rest of the paper is organized as follows: section 2 describes the Belt and its challenges;
 98 section 3 illustrates the theoretical basis for ANEMI_Yangtze; new aspects of the model
 99 development are provided in section 4; section 5 discusses the model validation and application;
 100 and section 6 offers the final conclusions.

101 **2. Yangtze Economic Belt: system description**

102 Yangtze river originates from the Tanggula Mountains on the Plateau of Tibet and flows
 103 eastward to the East China Sea. It has a total length of 6,300 km with a catchment area of about
 104 1.8 million km². Located mainly in the Yangtze river basin, the Belt traverses eastern, central and
 105 western China, joining the coast with the inland and consists of 3 economic zones – the Chongqing-
 106 Sichuan upstream urban agglomeration, the central triangle urban agglomeration, and the Yangtze
 107 river delta agglomeration, The relationship between the Yangtze river basin and the Belt is shown
 108 in Figure 1.



109 **The upstream urban agglomeration**

110 **Figure 1.** Yangtze river basin (black long dashed line) and the Yangtze Economic Belt

111 Over the past decades, especially after the reform and opening-up of China in the late 1970s,
 112 the Belt has developed into one of the most vital regions in China. It accounts for 21% of the
 113 country’s total land area (2.05 million km²) and is home to 40% of the country’s total population,

114 with an economic output exceeding 40% of the country's total GDP. The Belt is home to many
115 advanced manufacturing industries, modern service industries, major national infrastructure
116 projects, and high-tech industrial parks. As one of China's most important industrial corridors, the
117 Belt's output of steel, automobile, and petrochemical industries accounts for more than 36%, 47%,
118 and 50% of the total national output, respectively (MIIT, 2016). In 2018, the Belt's population and
119 GDP were about 599 million and 40.3 trillion RMB, accounting for 42.9% and 44.1% of the
120 country, respectively. As the initiation of the Belt in 2016 and the gradual loosening of China's
121 birth control policy, the Belt's processes of urbanization and industrialization are expected to gain
122 momentum in the coming decades (NDRC, 2016). The fast urbanization and strong economic
123 growth in the Belt, however, pose severe challenges for its sustainable development. These
124 challenges mainly include the climate change impacts, energy crisis, land availability and food
125 security, water pollution, and depletion of fish stock in the river.

126 **2.1 Climate change impacts**

127 The Yangtze river basin is vulnerable to global warming. Accumulating evidence shows that
128 climate change affects the hydrologic regime in the river basin. For example, research finds that
129 the glaciers in the Qinghai-Xizang Plateau in the head Yangtze regions shrank by 7% (3,790 km²)
130 over the past four decades (Li et al., 2010). This change in the hydrological cycle results in more
131 frequent extreme meteorological events happening in the Yangtze river basin (Cao et al., 2011; Gu
132 et al., 2015; Su et al., 2017), exposing vast majority of the population to growing physical and
133 socio-economic risks. For example, during the summer of 2020, eight provinces in the Yangtze
134 river basin experienced severe floods, leaving hundreds dead and disrupting the economy's post-
135 pandemic recovery.

136 **2.2 Energy crisis**

137 The Yangtze river basin is poor in fossil fuel endowments even though China's has the
138 world's largest coal reserves. Data from China Energy Statistical Yearbook indicates that in 2015
139 the Belt imported about 60% of its coal consumption (DENBS, 2016). The Yangtze river basin
140 has, however, abundant hydropower resources. It is estimated that the potential reserves of
141 hydropower resources in the Yangtze river basin are about 278 million kilowatts (Wang, 2015).
142 The Yangtze coastal areas are ideal locations for nuclear power construction. However, due to
143 technical limitations and development costs, coal still dominates energy consumption, accounting
144 for about 56% of total energy consumption currently (Su, 2019).

145 **2.3 Land availability and food security**

146 Statistics from the demographic yearbook indicate that the population in the Yangtze river
147 basin grew from 500 million in 1990 to about 600 million in 2020, and is expected to reach its
148 peak around 2030 if the one-child policy remains unchanged (Zeng and Hesketh, 2016). As the
149 country's birth control policy gradually loosens, the population in the Belt will grow even faster.
150 With a high population growth rate and rising income, the consumption of food, especially non-
151 starchy food such as dairy and meat, is expected to increase (Niva et al., 2020). This higher food
152 production has to come from the same amount of land or even less land due to the competing use
153 of land for urbanization. Population growth and urban expansion occupy many rich farmlands.
154 Research shows that from 2000 to 2015 urban areas in the Yangtze river basin increased by 67.51%
155 whereas cropland decreased by 7.53% (Kong et al., 2018).

156 **2.4 Water pollution**

157 The increasing application of fertilizers and pesticides in agriculture and discharging of
158 wastewater from a growing population and rapid industry development lead to severe problems
159 concerning pollution of freshwater, eutrophication of lakes, and deterioration of the water
160 ecosystem. Statistical data indicate that 86.9% of major lakes and 35.1% of major reservoirs in the
161 Yangtze river basin suffer from eutrophication (YRWRC, 2016). Among them, the most serious
162 case is the eutrophication of Lake Taihu, which is located in the floodplain of the lower Yangtze
163 river (Li et al., 2011). In 2007, the blue algal bloom outbreak in Lake Taihu cut off drinking water
164 supply for 2 million citizens in Wuxi city for a whole week (Qin et al., 2007). The last decade has
165 witnessed some 70 million RMB flowing into the eutrophication control of the Lake Taihu annually.

166 **2.5 Depletion of Yangtze fish stock**

167 Fishery resources in the Yangtze river are seriously depleted. To date, wild capture fisheries
168 production decreased to less than 100 thousand tonnes, falling well short of the maximum output
169 of 427 thousand tonnes in the 1950s (Zhang et al., 2020). The eggs and larvae of the four major
170 Chinese carps (the dominant commercial species in the Yangtze river) were approximately 1.11
171 billion in 2015, accounting for only 1% of historical production in 1965 (Yi et al., 1988; Zhang et
172 al., 2017). Habitat fragmentation and shrinkage as a result of reclamation of lakes for farmland
173 and dam construction, together with overfishing and water pollution, are the main factors
174 threatening aquatic biodiversity in the Yangtze river (Jiang et al., 2020; Zhang et al., 2020). In an
175 effort to protect Yangtze's aquatic life, a 10-year commercial fishing ban on the Yangtze was

176 introduced in 2020. Fishing in the main stream of Yangtze river, the Poyang-Dongting lakes, and
177 the seven major tributaries is temporarily banned for a period of 10 years starting from 2021.

178 **3. ANEMI_Yangtze: background and theoretical basis**

179 The ANEMI_Yangtze model currently consists of nine sectors: *Population, Economy, Land,*
180 *Food, Energy, Water, Carbon, Nutrients, and Fish.* It is developed based on the ANEMI3 global
181 model (Breach and Simonovic, 2021). The time horizon of the model is 2100 and the simulation
182 step is one year. By introducing a subscript variable, *location* (consists of upper, middle, and lower
183 Belt), we are able to build “one” model to account for the spatial heterogeneity within the Belt’s 3
184 economic zones – the upper Chongqing-Sichuan upstream urban agglomeration, the middle central
185 triangle urban agglomeration, and the lower Yangtze river delta agglomeration. The model is
186 grounded in systems thinking and developed using the system dynamics simulation approach.
187 System dynamics research originated in control engineering and is a valuable methodology for
188 capturing the nonlinearity, feedbacks, and delays in determining the dynamic behaviour of
189 complex systems (Forrester, 1961). In system dynamics, interactions and feedbacks between
190 system components illustrated using Causal Loop Diagram (CLD), are far more important for
191 understanding system behaviour than focusing on separate details (Sterman, 2000; Simonovic,
192 2009). In the following sections, we focus on illustrating the theoretical basis of the model. The
193 development of ANEMI_Yangtze is presented in section 4.

194 **3.1 Cross-sectoral interactions and feedbacks**

195 The cross-sectoral interactions and feedback in ANEMI_Yangtze (Figure 2) are discussed in
196 the following section. Capitalized italics are used for sector names and italics are used for names
197 of state variables.

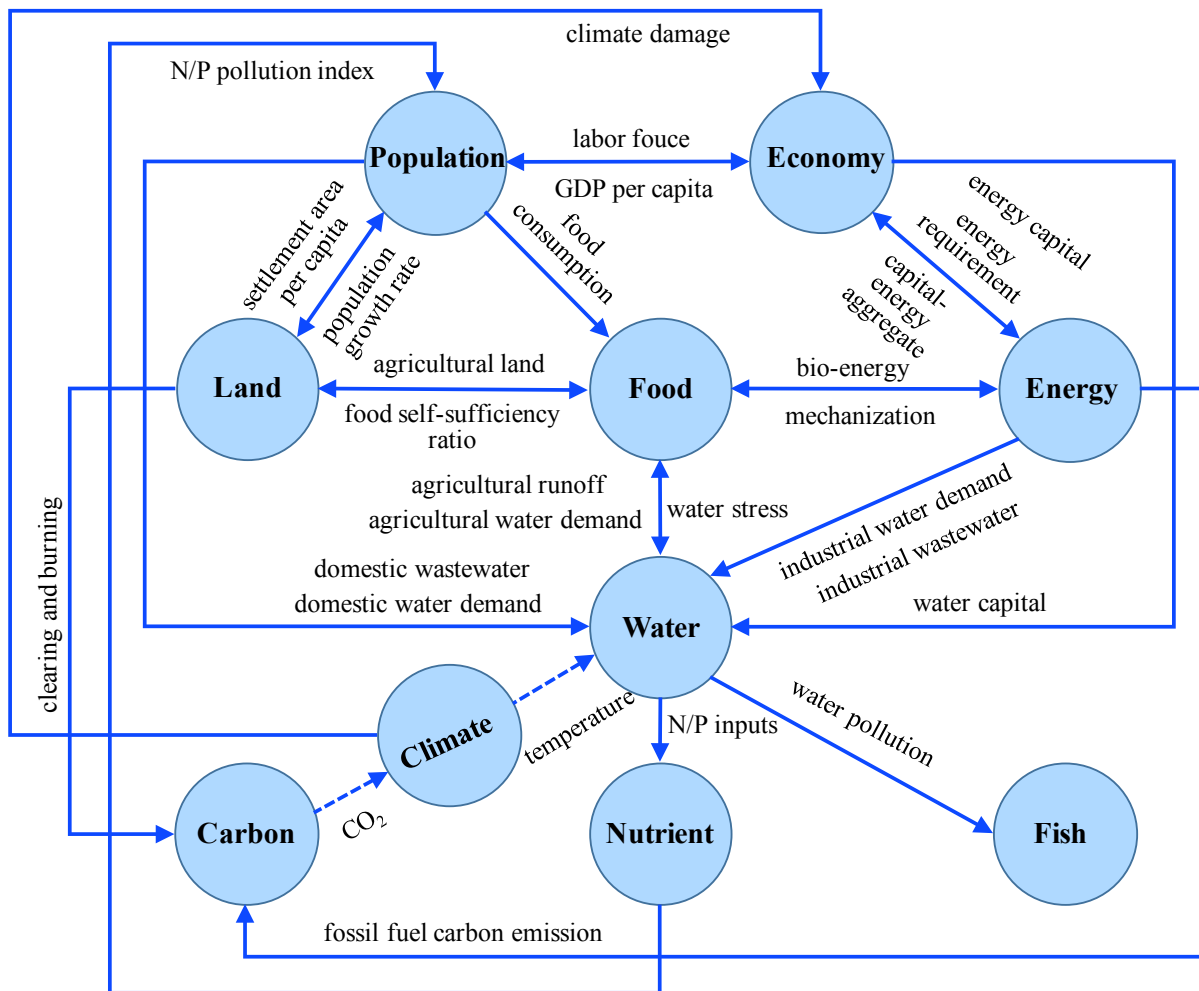


Figure 2. Cross-sectoral interactions among the human-natural systems in the Belt

198
199
200
201
202
203
204
205
206
207
208
209
210
211

The *Population and Economy Sectors* are linked through *GDP per capita* and *labour force*. *Population Sector* affects *Economy Sector* through *labour force*, an important element of the Cobb-Douglas production function. *Economy Sector* affects *Population Sector* both positively and negatively through *GDP per capita*. The reasoning behind this impact is that: increased *economic output*, on one hand results in higher quality health services and *life expectancy*, thereby reducing *mortality* rates; on the other hand, high housing price accompanied with economic development usually restrains fertility choices, thus reducing birth rates (Meadows et al., 1974; Dettling and Kearney, 2014; Breach, 2020). In China, the *total fertility* in more developed south-east regions is generally lower than in less developed western regions (Hui et al., 2012; Clark et al., 2020). In addition, the economic factor is the most important driver of migration (Lee, 1966). The differences in *GDP per capita* among the Belt's three economic zones affect population migration within the Belt.

212 The *Population, Food, and Land Sectors* are connected through *population growth rate, food*
213 *self-sufficiency ratio, and settlement area per capita*. Population growth accelerates the transfer
214 rate of biome among different land-use types (Goudriaan and Ketner, 1984). Population growth
215 drives *food consumption*, thereby decreasing *food self-sufficiency*, resulting in more agricultural
216 land being converted by clearing and burning forests and grassland. Population growth also leads
217 to more agricultural land around the urban area be claimed for settlement use as urban expands.
218 The *Land Sector* negatively impacts population growth as increased population places more stress
219 on *settlement area per capita*, which then acts as an opposing force on the migration rate (this
220 feedback is further clarified in section 4.3).

221 The *Economy and Energy Sectors* are linked through *capital-energy aggregate, energy*
222 *capital, and energy requirement*. A growing economy increases the need for energy, which drives
223 *energy production* through increasing *energy capital* investment. An increase in *energy capital*
224 further intensifies the *capital-energy aggregate*, driving economy growth, thus forming a positive
225 feedback loop.

226 The *Population, Food, Energy, and Water Sectors* are connected via *domestic water demand*
227 *and consumption, agricultural water demand and consumption, and industrial water demand and*
228 *consumption*. Water (irrigation) plays a vital role in food production and is needed in almost every
229 stage of energy extraction, production, processing, and especially consumption. With increased
230 population and demand for food and energy, the total demand for and consumption of water
231 increases, increasing *water stress*, which in turn, impedes population growth and *food production*
232 (Dinar et al., 2019; Breach, 2020). The increasing *water stress* also drives more capital flowing
233 into water supply development so as to alleviate *water stress*, thus connecting the *Economy* sector
234 with the *Water Sector*.

235 The use of water by *Population, Energy, and Food Sectors* all result in water pollution in the
236 form of increased nutrient concentration through the discharge of *domestic and industrial*
237 *wastewater and agricultural runoff*. This links the *Water Sector* with the *Nutrient Sector*. An
238 increased level of *nutrient concentration* negatively affects population growth through the *life*
239 *expectancy multiplier* (Pautrel, 2009), thus links the *Nutrient-Population Sectors*. Water pollution
240 also endangers fish by increasing the population's *natural mortality rate* (Zhang et al., 2020).

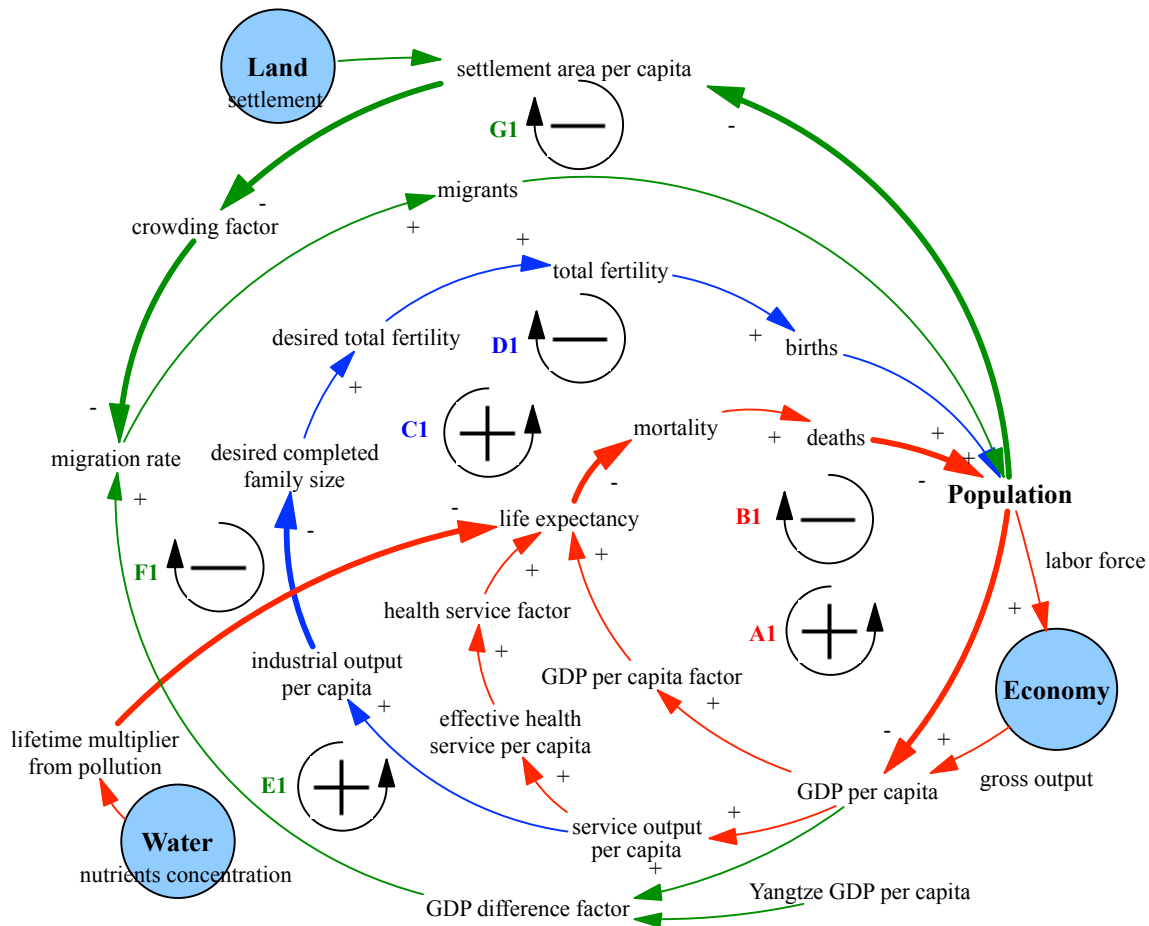
241 The *Carbon and Land Sectors* are connected through clearing and burning, while the *Carbon*
242 and *Energy Sectors* are connected through *fossil fuel emissions*. The *Carbon-Climate* sector

243 feedback depends on the atmospheric CO₂ concentration determined by the *Carbon* sector. The
244 climate change effect is treated as exogenous input. The *Climate* and *Water Sectors* are connected
245 via the *surface temperature change*. Since increased surface temperature will likely increase the
246 intensity of the hydrological cycle (Giorgi et al., 2011), the model includes a temperature multiplier
247 equation that increases evaporation and evapotranspiration within the Yangtze hydrological cycle.
248 The *Climate Sector* influences the *Economy* sector through a temperature damage function,
249 developed by Nordhaus and Boyer (2000).

250 **3.2 Interactions and feedbacks within model sectors**

251 **3.2.1 CLD in the *Population Sector***

252 The three variables - *births*, *deaths*, and *migrants*, which are all affected by *GDP per capita*,
253 drive the dynamic behaviour of the population in the Belt. *GDP per capita*, which is affected by
254 *labour force* (population) and *gross output*, rises if the effect of the increase in the *gross output*
255 outpaces the effect of the population increase, and vice versa. So, the feedback loops containing
256 *GDP per capita* can either be positive or negative depending on whether *GDP per capita* is
257 increasing or decreasing with population growth. Figure 3 shows the feedbacks in the *Population*
258 *Sector*. The positive loop A1 and negative loop B1 depict the effect of *GDP per capita* on mortality,
259 whereas positive loop C1 and negative loop D1 have the effect on fertility. The positive loop E1
260 and negative loop F1 illustrate the impact of *GDP difference factor* on migration, whereas loop
261 G1 explains the effect of crowding on migration. The process of and the mechanism behind the
262 CLD are illustrated in sections 3.1 and 4.3.



263

264

Figure 3. CLD in the *Population Sector*

265

3.2.2 CLD in the *Economy Sector*

266

267

268

269

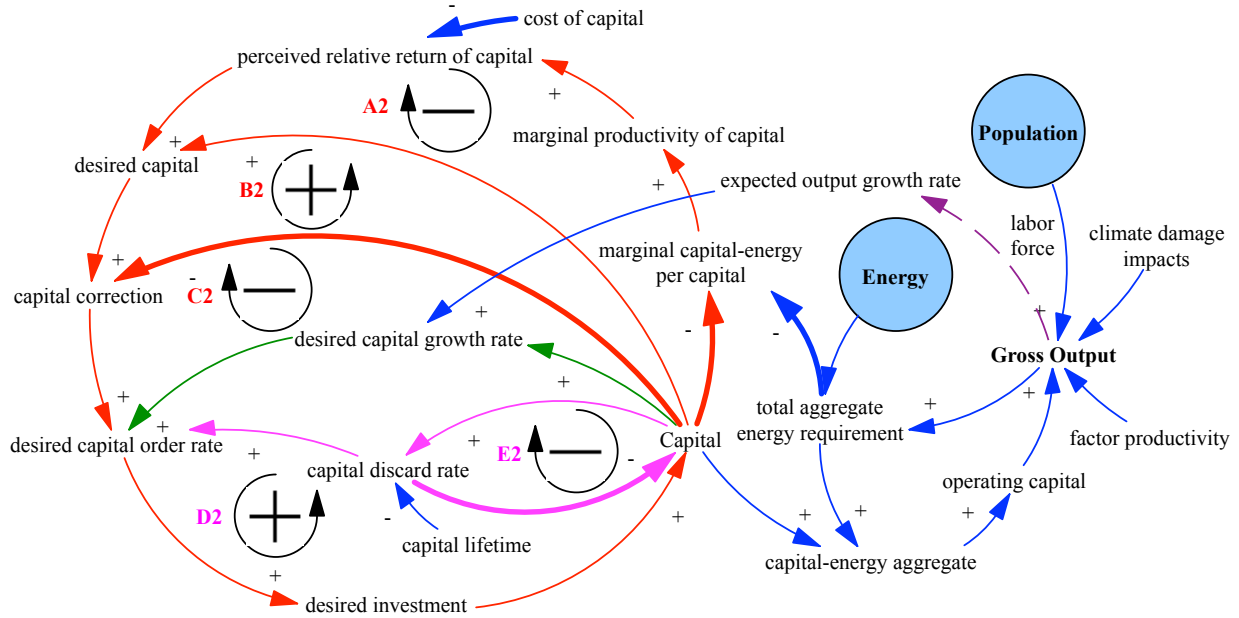
270

271

272

273

The interactions and feedbacks in the *Economy Sector* are presented in Figure 4. Capital orders respond to three pressures. Orders first replace depreciation (loops D2 and E2). Loop E2 depicts the process of depreciation, which slowly depletes the *capital* stock. Loop D2 compensates for depreciation by factoring it into *desired capital order rate*. Orders then correct the gap between desired and actual capital (loop C2). The *desired capital* stock is anchored on the real *capital* stock and adjusted for the relative cost and *marginal product of capital* (loops A2 and B2). Finally, orders augment the *capital* stock in order to anticipate output growth. See also Fiddaman (1997) and Breach (2020) for a detailed process of and mechanism behind the CLD in the *Economy Sector*.



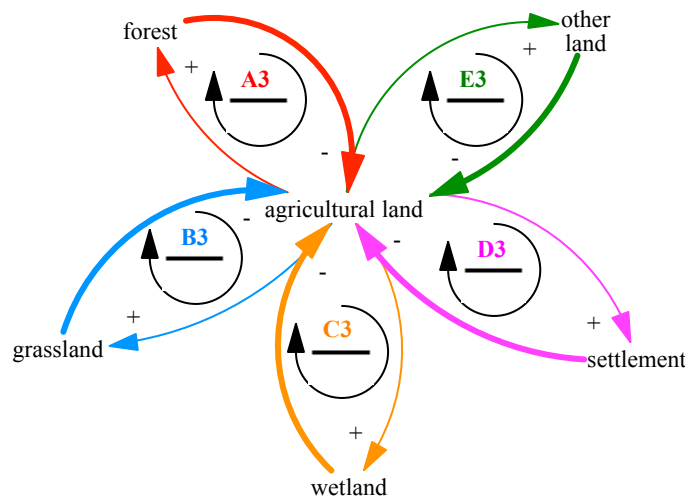
275

276

Figure 4. CLD in the *Economy Sector*

277 **3.2.3 CLD in the *Land Sector***

278 Figure 5 illustrates the feedbacks in *agricultural land* (the feedback loops in the *forest*,
 279 *grassland*, *wetland*, *settlement*, and *other land*, which are not shown in the figure, are the same as
 280 those in the *agricultural land*). An increase in the stock of *agricultural land* increases its transfer
 281 rate to the *forest*, *grassland*, *wetland*, *settlement*, and *other land*, which all together drain the stock
 282 of *agricultural land* and form the negative loops A3, B3, C3, D3, and E3.



283

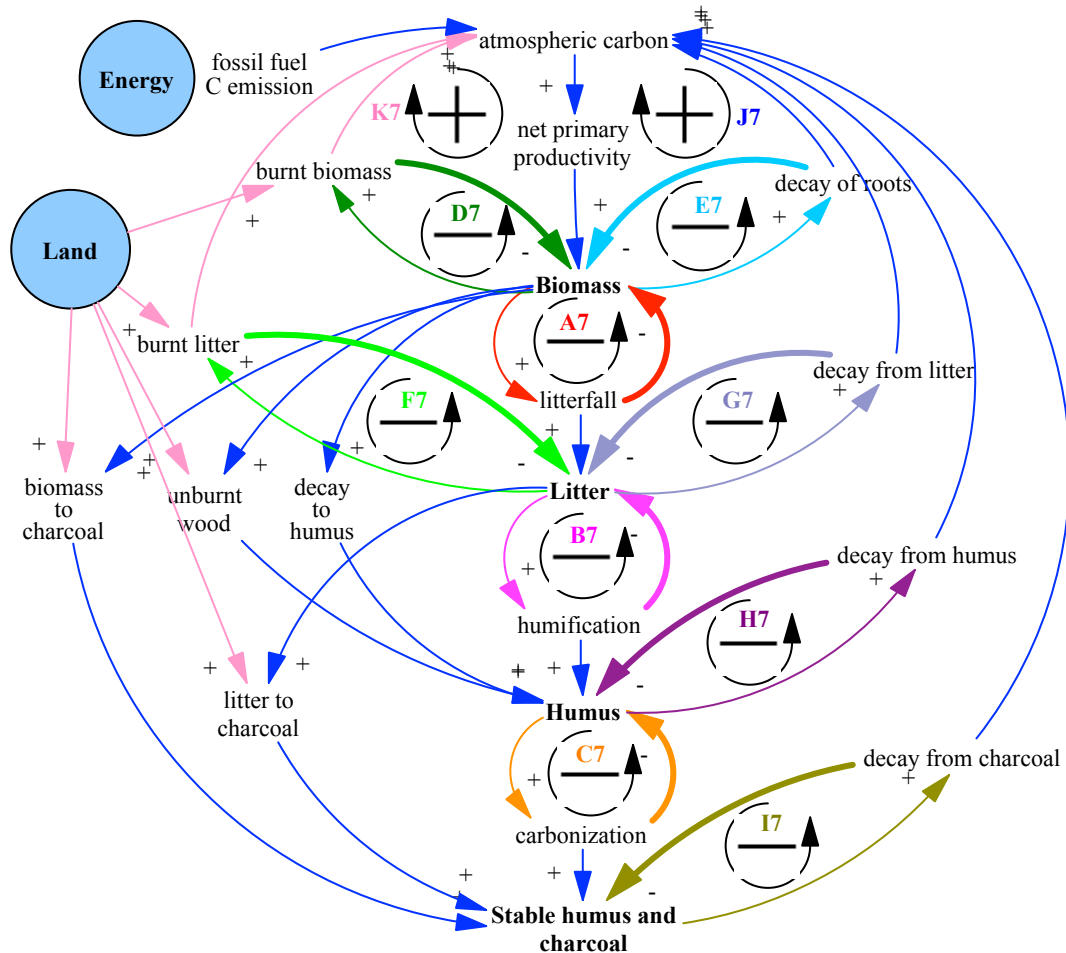
284

Figure 5. CLD in the *agricultural land*

285 **3.2.4 CLD in the *Food Sector***

286 The CLD in the *Food Sector* is shown in Figure 6. Negative loops A4, B4, and C4 illustrate
287 the impacts of *land yield technology*, *agricultural land development*, and *fertilizer subsidy*,
288 respectively, on *food production* through the indicator of *food self-sufficiency ratio*. A decrease in
289 *food self-sufficiency ratio* stimulates inputs in *land yield technology*, *agricultural land*
290 *development*, and *fertilizer subsidy*, which all drive up *land yield*, resulting in increases in *food*
291 *production* and *food self-sufficiency ratio* (Ju et al., 2020). The changes or fluctuations in
292 agricultural product prices are widely recognized as significant factors driving grain production
293 (Xie and Wang, 2017). Negative loops E4 and F4 depict the introduction of multiple cropping
294 practices (*multiple cropping index*) and *willingness to increase grain planting area* on *food*
295 *production* through *food price change*. An increase in *food price change* acts as positive feedback
296 on farmers' adopting of multiple cropping practices (*multiple cropping index*) and increasing *grain*
297 *planting area*. Positive loop D4 counterbalances the effect of adopting multiple cropping practices
298 by decreasing *land fertility* and the corresponding *land yield*.

345 atmosphere. See also Goudriaan and Ketner (1984), Davies and Simonovic (2010, 2011), and
 346 Breach (2020) for the detailed mechanism behind the CLD in the *Carbon Sector*.
 347



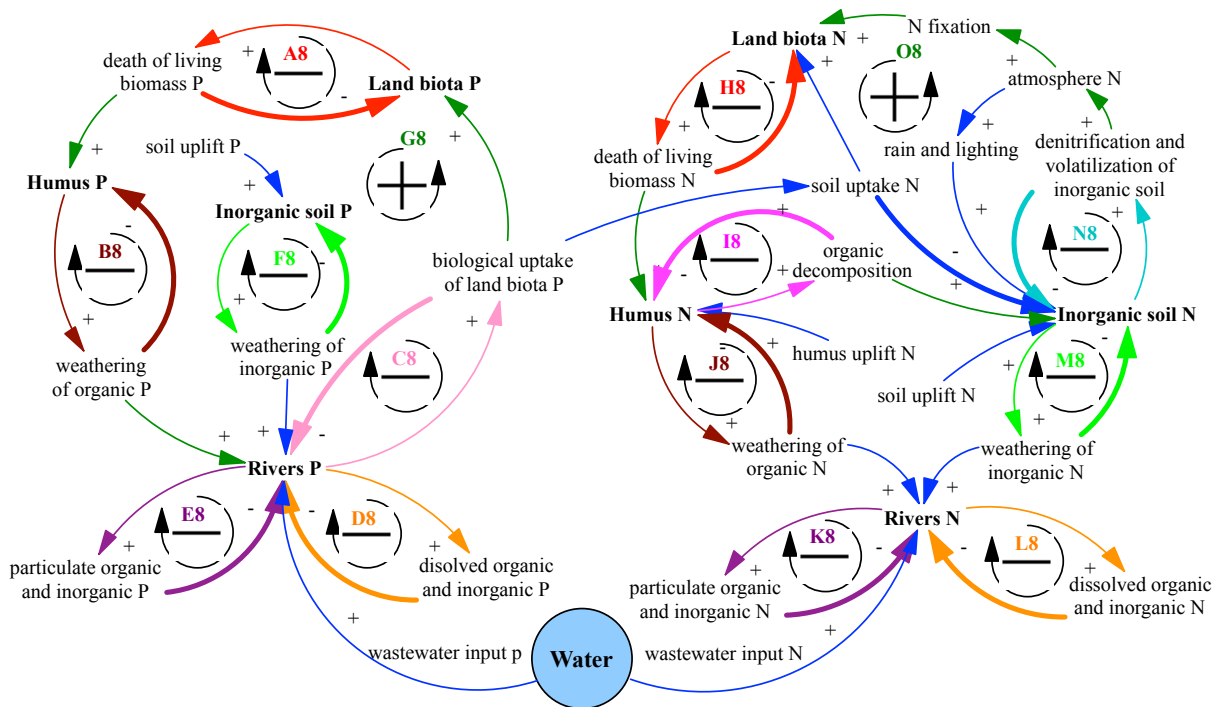
348
 349 **Figure 9. CLD in the *Carbon Sector***

350 **3.2.8 CLD in the *Nutrient Sector***

351 The CLD in the *Nutrients Sector* is given in Figure 10. The cycles of phosphorous and
 352 nitrogen follow that of the carbon cycle. Take a phosphorous cycle for example, the chain of
 353 negative feedback loops passing through *land biota* to *humus* and to *rivers* (A8, B8, C8, D8, E8)
 354 and the negative feedback loops depicting the *weathering of inorganic P* (F8) act as a positive
 355 feedback loop in the terrestrial phosphorous cycle (G8). Because it represents a continuous cycle
 356 of negative feedback, it will attempt to reach equilibrium under natural conditions. Anthropogenic
 357 influences on this system in the form of wastewater discharge affect this equilibrium and drive

358 change in the nutrient cycles. See also Mackenzie et al. (1993) and Breach (2020) for the detailed
 359 mechanism behind the CLD in the *Nutrient Sector*.

360



361

362

Figure 10. CLD in the *Nutrient Sector*

363 3.2.9 CLD in the *Fish Sector*

364 Four feedback loops drive the dynamics of *fish biomass stock* (see Figure 11). Loops A9, C9,
 365 and D9 represent negative feedback on *fish biomass stock* through *natural fish death*, *fish recruits*,
 366 and *fish yield*, respectively. The amount of wastewater water acts as a positive factor on *natural*
 367 *mortality*. Loop B9, which connects *total reservoir capacity* and *ship cargo volume* with *fish birth*
 368 *rate*, acts as positive feedback on *fish biomass stock*. As the *total reservoir capacity* and *ship cargo*
 369 *volume* increase, the *fish birth rate* decreases so too does the *fish birth*. The decline in *fish birth*
 370 decreases the *fish biomass stock*, further reducing the *fish birth*.

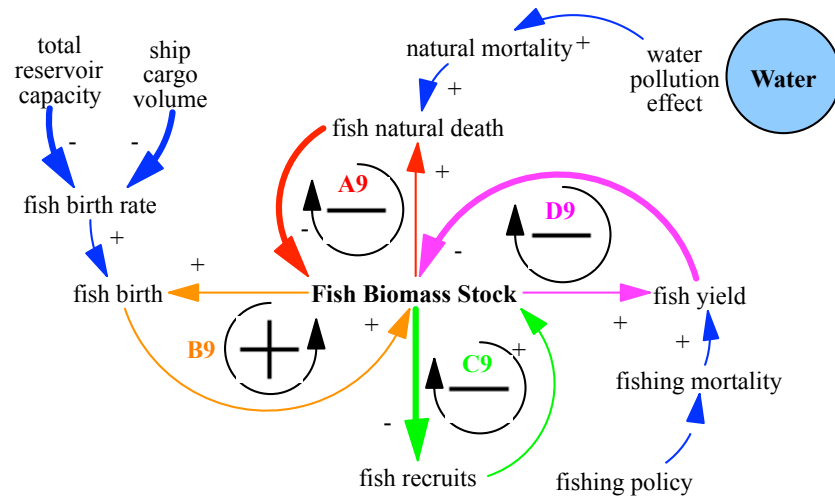


Figure 11. CLD in the *Fish Sector*

4. ANEMI_Yangtze: model development

4.1 The ANEMI_Yangtze data system

The ANEMI_Yangtze data system contains (i) historical data that is used to initialize and validate the model and (ii) future parameters that govern changes in the future. Most of the historical data (1990-2015), such as population and GDP, energy production and consumption, food production and food trade, and water withdrawals and consumptions, come from the Statistical Yearbook published by the National Bureau of Statistics of China annually (also available on line at <http://www.stats.gov.cn/english/>, last accessed Sep 20, 2021). Historical precipitation, evapotranspiration, and temperature data are collected from hydrometeorological stations. Land use data come from ESA Climate Change Initiative - Land Cover (<http://maps.elie.ucl.ac.be/CCI/viewer/>, last accessed Sep 20, 2021). Adjustments are made to the historical data as needed to fill in the missing information. Future temperature and precipitation data come from Yu et al (2018). For the future parameters, the ANEMI_Yangtze data system uses information about technology cost and performance, information about future development policies, as well as the authors' experience of knowledge. Additional information on the data is also described in the sections below.

4.2 Major changes: a glimpse

The ANEMI_Yangtze is developed based on ANEMI3, which has its roots in the *WorldWater* by Simonovic (2002; 2002a). ANEMI has been updated continuously from its first publication in 2010 (Davies and Simonovic, 2010) to the most recent edition in 2021 (Breach and Simonovic, 2021). The current version of ANEMI consists of the following twelve sectors that reproduce the

394 main characteristics of the climate, carbon, population, land use, food production, sea-level rise,
 395 hydrologic cycle, water demand, energy-economy, water supply development, nutrient cycles, and
 396 persistent pollution. In the ANEMI_Yangtze, the hydrological cycle, water demand and water
 397 supply development, as well as wastewater discharge and treatment, are all integrated in the *Water*
 398 *Sector*. Climate change is not explicitly simulated. Instead, we use exogenous precipitation and
 399 temperature to drive the *Water Sector*'s hydrological cycle. Sea level rise and persistent pollution
 400 are excluded. The global cycles of carbon, nutrients, and hydrology are tailored to fit a regional
 401 context. A new *Fish Sector* is added since fisheries are important for the regional economy and
 402 diet. Major modifications are in the *Population*, *Food*, *Energy*, and *Water Sectors*. Due to space
 403 limitation, only new aspects of the model are described in detail. For further information about the
 404 model, please also refer to ANEMI_Yangtze's technical report from Jiang and Simonovic (2021)
 405 and Dr. Breach's PhD dissertation (Breach, 2020).

406 4.3 Population

407 *Births*, *deaths*, and *migrants* are the three variables drive the dynamic behaviour of the Belt's
 408 population. Figure 12 shows the stock and flow diagram in the *Population Sector*. Population is
 409 split into three age demographics to allow for the working population (ages 15 to 64) to represent the
 410 *labor force* in the economic model. The ageing chain of population groups can be represented as:

$$411 \begin{cases} P_{0-14} = \int \left(B + netM_{0-14} - P_{0-14} \cdot M_{0-14} - \frac{P_{0-14}(1-M_{0-14})}{\tau_1} \right) dt \\ P_{15-64} = \int \left(netM_{15-64} + \frac{P_{0-14}(1-M_{0-14})}{\tau_1} - P_{15-64} \cdot M_{15-64} - \frac{P_{15-64}(1-M_{15-64})}{\tau_2} \right) dt \\ P_{65+} = \int \left(netM_{65+} + \frac{P_{15-64}(1-M_{15-64})}{\tau_2} - P_{65+} \cdot M_{65+} \right) dt \end{cases} \quad (1)$$

412 Where P_i is population, $netM_i$ is *net migrants*, M_i is *mortality*, τ_i is length of time spent in sub-
 413 demographic. B represents *births* and is calculated as,

$$414 B = TF \cdot \frac{FM_r \cdot P_{15-49}}{R_{life}} \quad (2)$$

415 Where FM_r is *female ratio* (its value usually lower than 0.5 due to the well-known phenomenon
 416 of "missing girls", a side-effect of the one-child policy), P_{15-49} is the population between age 15-
 417 49, R_{life} is *reproductive lifetime* of 30 years. TF is *total fertility*, which is determined by a number
 418 of factors, including *fertility control effectiveness*, capital allocation, and *desired family size*. Its
 419 calculation (equation (3)) is adapted from ANEMI3 (Breach, 2020).

$$420 TF = MIN(MTF, (MTF \cdot (1 - F_{control}) + DTF \cdot F_{control})) \quad (3)$$

421 where TF is *total fertility*, MTF is *maximum total fertility*, $F_{control}$ is *fertility control effectiveness*,
 422 DTF is *desired total fertility*.

423 *Life expectancy*, which determines *mortality*, is affected by both economic and environmental
 424 factors. The calculation of *life expectancy* is adapted from Ma and Yu (2009). At the regional scale,
 425 vital resources such as food and water can be traded, so in ANEMI_Yangtze, only the effect of
 426 pollution is incorporated in the equation for *life expectancy* as a multiplier. The empirical
 427 relationship between *mortality* and *life expectancy* is adopted from ANEMI3 which originally
 428 adopts from Meadows et al. (1974).

$$429 \quad L_E = (L_{EN} + a \ln GDP_{per} + b \ln EHS_{per}) Pollution_{multi} \quad (4)$$

$$430 \quad Pollution_{multi} = c \cdot PI^2 + d \cdot PI + e \quad (5)$$

$$431 \quad PI = \sqrt{\frac{N_I}{N_{I0}} \cdot \frac{P_I}{P_{I0}}} \quad (6)$$

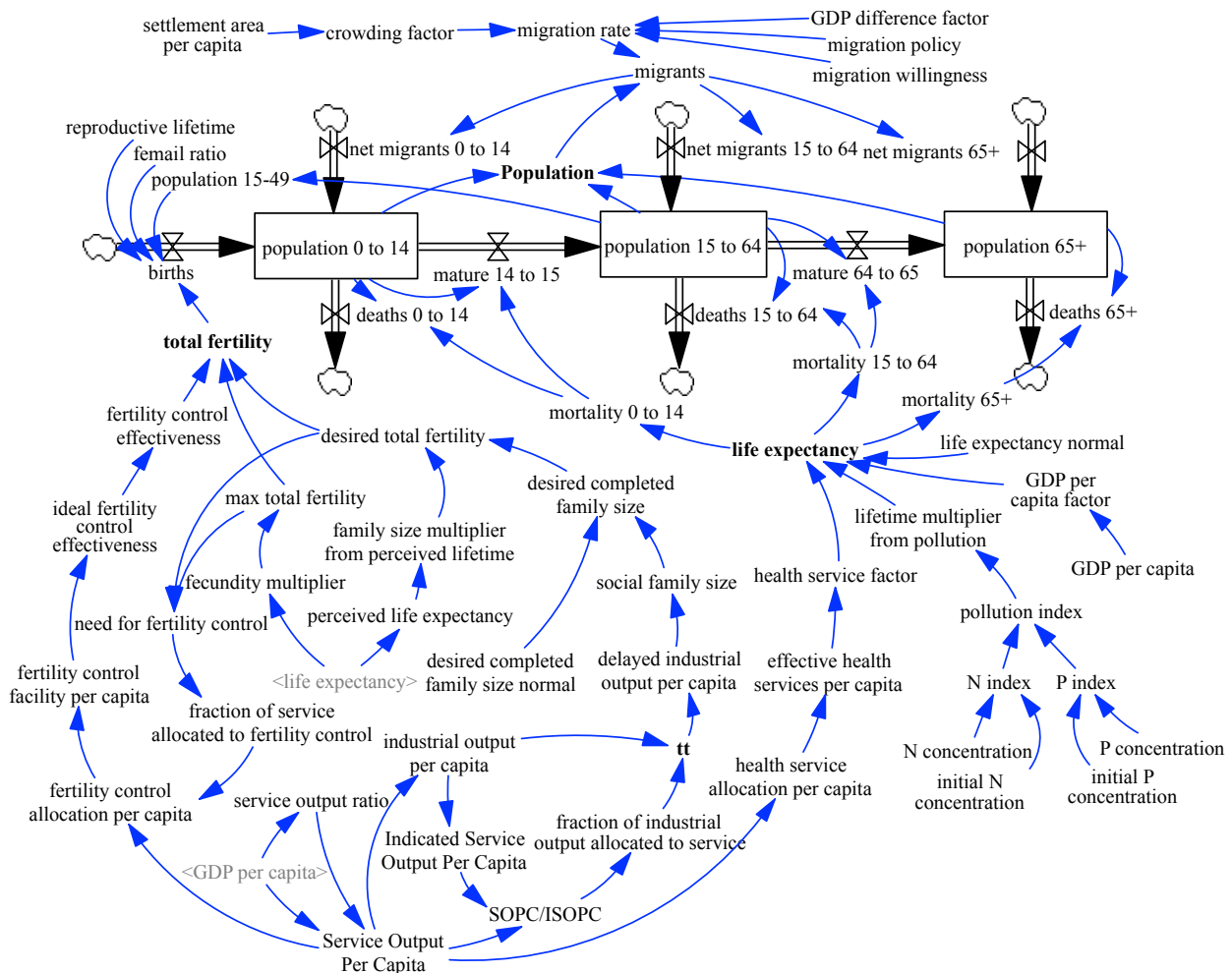
432 Where L_E is *life expectancy*, L_{EN} is *life expectancy normal*, GDP_{per} is *GDP per capita*, EHS_{per} is
 433 *effective health service per capita*, $Pollution_{multi}$ is *lifetime multiplier from pollution*, PI is *pollution*
 434 *index*. $N_I (P_I)$ and $N_{I0} (P_{I0})$ are the simulated and initial nitrogen (phosphorous) concentration. a ,
 435 b , c , d , and e are calibrated parameters.

436 Migration is newly added. According to Lee (1966), labor migration is caused by the wage
 437 difference between immigration and emigration, and economic factors are the main factor affecting
 438 migration and mobility. For China, the most important factor driving migration in the 1980s (post-
 439 reform period) is the institutional driver and then the economic driver dominants after that (Shen
 440 2013). Apparently, the effect of migration policy can't be ignored considering China's central-
 441 planning logic and mechanisms when studying the Belt's migration. We introduce a *migration*
 442 *policy* factor to account for the institutional barrier and suppose its value ranges from 0-1, with
 443 bigger value indicating policy that is in favor of migration. Social environment is also an
 444 intermediate factor affecting migration (Lei et al., 2013). In China, most minorities (China's 56
 445 ethnic groups) live in areas with the same or similar language and culture as well as eating habits
 446 and are very reluctant to move (Su et al., 2018). Therefore, we employ a factor - *migration*
 447 *willingness* - which is calculated as the proportion of the minorities to account for the "border
 448 effect" in migration. In addition, research also has that economic prosperity on the one hand,
 449 attracts labour migration, on the other hand, restrains population inflows in the megacities due to
 450 high housing prices (Zhao and Fan, 2019). This research introduces a *crowding factor* affected by

451 settlement area per capita to account for house price impact. The calculation of migration rate
 452 MR is thus formulated as:

453
$$MR = F_{GDP\ diff} \cdot MW \cdot MP \cdot F_{crowding} \quad (7)$$

454 where $F_{GDP\ diff}$ is GDP difference factor, which is used to calculate the difference between GDP
 455 per capita in the upper, middle, and lower Yangtze Economic Belt and GDP per capita in the Belt.
 456 This means only the migration within the Belt is considered (i.e., people migrate from the less
 457 developed upper and middle Belt to the developed lower Belt) and the migration between the Belt
 458 and the rest of China is ingored. MW is migration willingness. MP represents migration policy and
 459 the value of 1 is adopted in this research. $F_{crowding}$ is a crowding factor and is affected by settlement
 460 area per capita.



461

462

463

Figure 12. Stock and flow diagram of the *Population Sector*

4.4 Food

464 The *Food Sector* of ANEMI_Yangtze calculates the production and consumption of food and
 465 *food import/export*, and its stock and flow diagram is shown in Figure 13. *Food consumption* is
 466 the production of *population* and *per capita food consumption*. In ANEMI_Yangtze, *per capita*
 467 *food consumption* is assumed to be 400 kg/year/person throughout the simulation. *Food production*
 468 is affected by several factors, including *land fertility*, *arable land*, and *water stress*. Its dynamic
 469 behaviour is mainly driven by the difference between *perceived food self-sufficiency* and *desired*
 470 *food self-sufficiency*. The *food self-sufficiency* index is defined as the ratio of *food production* to
 471 *food consumption*. When its value declines below 0.95 (a critical value) incentives for *land yield*
 472 *technology input*, *agricultural land development*, and *fertilizer subsidy* shall be provided to ensure
 473 food security (Ye et al., 2013).

$$474 \quad FP = LY \cdot GPA \cdot (1 - Loss) \quad (8)$$

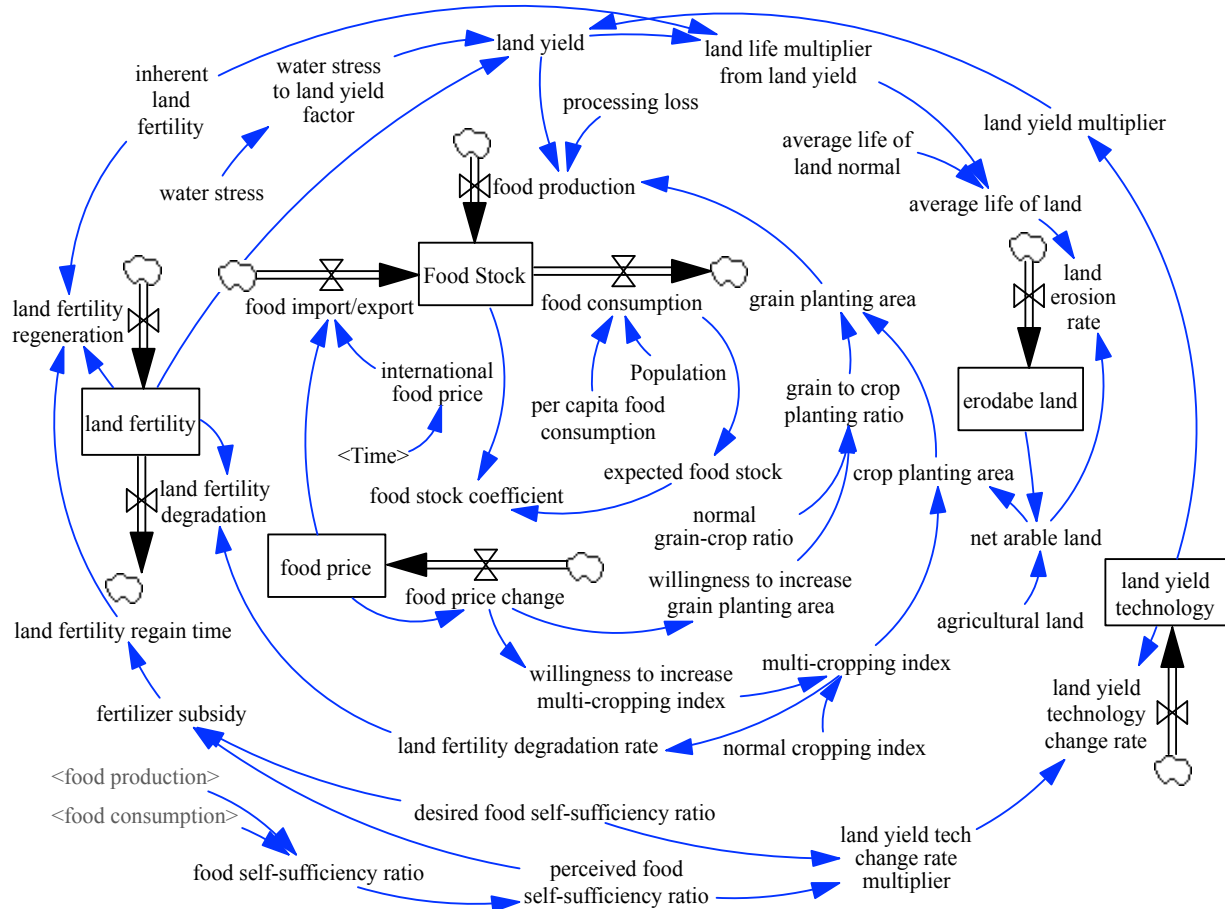
$$475 \quad LY = LF \cdot LY_{multi} \cdot F_{WS} \quad (9)$$

476 where *FP* is *food production*, *LY* is *land yield*, *GPA* is *grain planting area*, *Loss* represents
 477 *processing loss*. *LF* is *land fertility*, *LY_{multi}* is *land yield multiplier*, *F_{WS}* represents *water stress to*
 478 *land yield factor*.

479 The *Food Sector* also enables food trade, *i.e.*, *food import* and *food export*, which is affected
 480 by *local food price* and *international food price* and its calculation is adapted from Wang et al.
 481 (2009).

$$482 \quad FIE = F_{pop} \cdot f_1 + f_2 \cdot FP - f_3 \cdot IFP \quad (10)$$

483 Where *FIE* is *food import/export*, with positive *FIE* indicating import and negative ones export.
 484 *F_{pop}* is population rescale factor, approximately equals to the ratio of the Belt's population to the
 485 national total population. *FP* is *food price* and *IFP* is *international food price*. The historical values
 486 of *IFP* are from FAO (<http://www.fao.org/worldfoodsituation/foodpricesindex/en/>, last accessed
 487 Sep 20, 2021). The future values of *IFP* are set to the base year 2015 values. *f_i* are calibrated
 488 parameters. *Food price* is simulated as a stock variable and accumulates by *food price change*,
 489 which is another important factor affecting *food production* through influencing farmers' adopting
 490 of multiple cropping practices (*multiple cropping index*) and increasing *grain planting area*.



491

492

Figure 13. Stock and flow diagram of the *Food Sector*

493 4.5 Energy

494

495

496

497

498

499

500

501

502

503

504

The energy system of ANEMI_Yangtze includes the representation of *energy capital* development, *energy technology*, and *energy requirement, production, and consumption*. Figure 14 shows the stock and flow diagram of the *Energy Sector*. Six primary energy resources, three renewable sources (hydropower, nuclear, and new energy sources) and three non-renewable sources (coal, oil, and gas) are considered. *Energy capital* is energy production capital stock. It is represented as developed field or mine for fossil fuels and built plants for nuclear and hydropower. The formulations of *energy capital* (KE_i) and *energy capital under construction* (KEC_i) are the same as those in ANEMI3 (Breach, 2020: equations (3.52), (3.53)). For simplicity, we do not simulate the effect of return on *energy capital* which is determined by energy capital cost and the marginal product of energy capital in ANEMI3. We thus formulated the calculation of *desired energy capital order rate* as,

$$505 \quad DKEO_i = \frac{KE_i}{\delta_i} + \frac{DKE_i - KE_i}{\tau_c} + \frac{DKEC_i - KEC_i}{\tau_s} \quad (11)$$

$$506 \quad DKEC_i = \frac{KE_i}{\delta_i} + GR_{GDP} \cdot KE_i \cdot delay_c \quad (12)$$

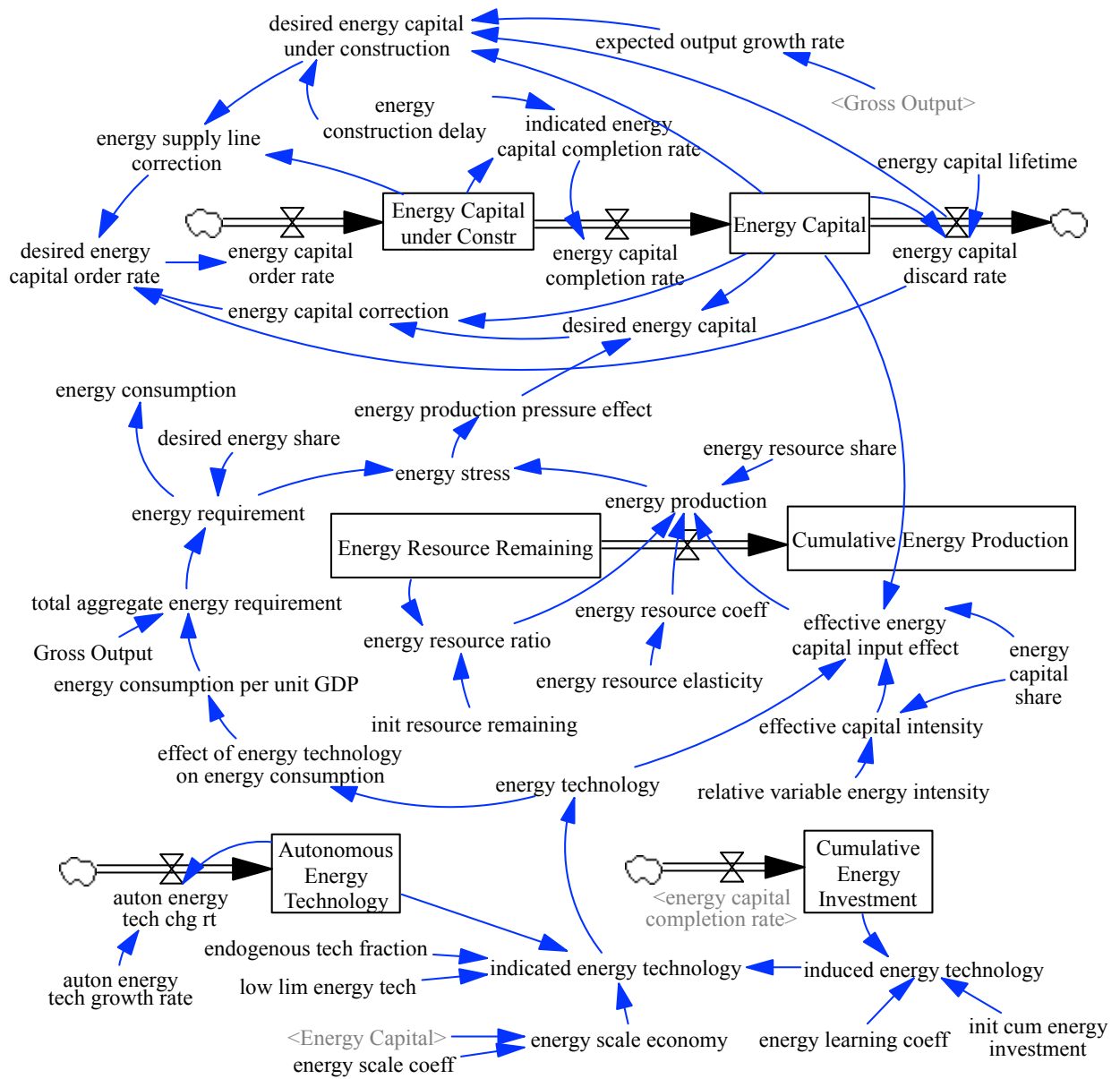
507 The first term on the right-side of the formula represents *energy capital discard rate* in which KE_i
 508 is *energy capital*, δ_i is *energy capital lifetime*. The middle term represents *energy capital*
 509 *correction* in which DKE_i is *desired energy capital*, equaling to current *capital* adjusted for
 510 *production pressure*. The pressure effect of energy production is treated as a look-up table function
 511 of *energy stress*. *Energy stress* is defined as the ratio of *energy requirement* to *energy production*.
 512 τ_c is correction time for *energy capital*. The third term represents correction to supply line of
 513 *energy capital under construction* in which $DKEC_i$ and KEC_i are desired and current *energy capital*
 514 *under construction*. $DKEC_i$ equals quantity needed to replace discards and meet growth and is
 515 formulated as equation (12), in which GR_{GDP} is expected growth rate of *gross output*, $delay_c$
 516 represents the time required to construct new *energy capital*. τ_s is correction time for supply line
 517 of *energy capital under construction*. i denotes the six energy sources.

518 The *total aggregate energy requirement* in ANEMI_Yangtze scales with economy and is
 519 represented as the production of *gross output* and *energy consumption per unit GDP*. *Energy*
 520 *requirement* by sources is the production of *total aggregate energy requirement* and *desired energy*
 521 *share* (which is exogenously specified in this research).

522 Three factors affect *energy production* for each source: *energy capital*, *energy technology*,
 523 and resources effect. The supply of producing capital is mainly driven by the pressure effect of
 524 energy production, *i.e.*, *energy stress* (defined as the ratio of *energy requirement* to *energy*
 525 *production*). Resource effect affects *energy production* through depletion and saturation. The
 526 depletion effect represents the diminishing productivity of nonrenewable energy production as the
 527 resource remaining declines and saturation refers to diminishing returns to production effort for
 528 the renewable energy. Technology increases *energy production* for the same level of inputs of
 529 *energy capital* through learning process usually called as an endogenous learning curve, with
 530 cumulative investment in *energy capital* as its input. The formulation of *energy production* is the
 531 same as in ANEMI3 (Breach, 2020: equations (3.49)) which is based on Fiddaman (1997).

532 *Energy price* in ANEMI3 is endogenously simulated, whereas in ANEMI_Yangtze it is
 533 exogenously specified, with historical prices from China Customs Head Office and China Energy
 534 Statistical Yearbook and future prices assumed to remain their 2015 base year values.

535 *Energy consumption equals to energy requirement by assuming that requirement can always*
 536 *be met through production and trade. Energy trade is not simulated in this research.*



537
 538 **Figure 14.** Stock and flow diagram of the *Energy Sector*

539 Table 1 shows the endowments of the six energy sources. Reserves for renewables mean the
 540 upper limit to renewable output. The upper limit for hydropower is based primarily on the hydro
 541 endowment, nuclear potential implicitly assumed to be politically limited, and new energy is the
 542 sum of wind and solar potentials.

543 Table 1 Energy endowments in the Belt

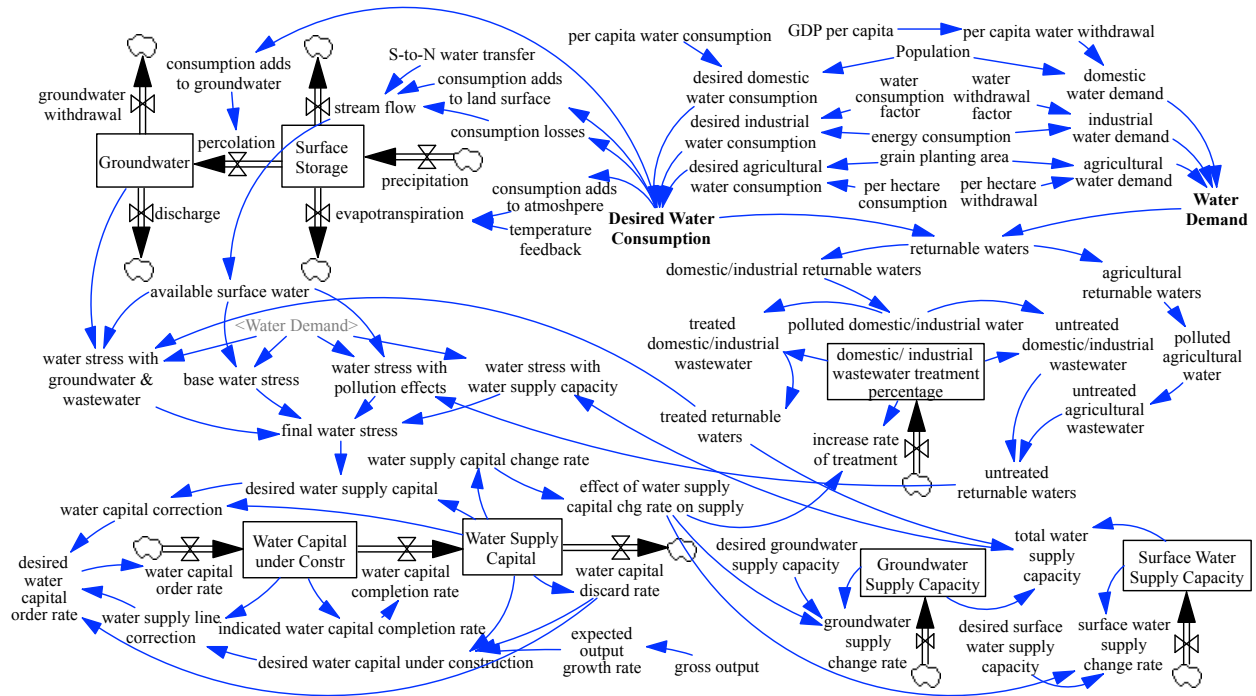
Type	Energy source	Reserves	Unit	Source
------	---------------	----------	------	--------

non-renewables	coal	128.556	billion tce	Yao et al. 2020
	oil	0.460	billion tce	Fang et al. 2018
	gas	19.188	billion tce	Fang et al. 2018
renewables	hydropower	0.379	billion tce/year	Liu and Ding, 2013
	nuclear	0.134	billion tce/year	SGERI and CNPD 2019
	new	318.386	billion tce/year	Song 2013; Zhu et al. 2006

544

545 4.6 Water

546 *Water Sector* consists of the hydrological cycle, *water demand*, *desired water consumption*,
 547 water supply development, as well as wastewater discharge and treatment. Figure 15 shows the
 548 stock and flow diagram of the *Water Sector*.



549

550 **Figure 15.** Stock and flow diagram of the *Water Sector*

551 The hydrological cycle describes the flow of water from the atmosphere in the form of
 552 *precipitation* to the land *surface storage* and through the *groundwater* back to the East China Sea.
 553 The South-to-North water transfers (west line, middle line, and east line) and *water consumption*
 554 are also taken into account. The water balance equations in the Belt are as follows,

$$555 \quad SS = \int (Pre - ET - Per - SF) dt \quad (13)$$

$$556 \quad GW = \int (Per - GWW - Dis) dt \quad (14)$$

$$557 \quad Per = a \left(\frac{SS}{SS_0} \right) + CS_{gr} \quad (15)$$

558
$$SF = b\left(\frac{SS}{SS_0}\right)^2 - CS_{at} - CS_{ls} - CS_{gr} - CS_{loss} - S2N \quad (16)$$

559
$$Dis = c\left(\frac{GW}{GW_0}\right) \quad (17)$$

560 Where *SS* is *surface storage*, *Pre* is *precipitation*, *ET* is *evapotranspiration*. *Per* and *SF* represent
 561 *percolation* and *stream flow* and are formulated as equations (15) and (16), respectively. *CS_{at}*, *CS_{ls}*,
 562 *CS_{gr}*, and *CS_{loss}* represent respectively the *water consumption adds to atmosphere*, *landsurface*,
 563 *groundwater*, and *consumption loss*. *S2N* is the South-to-North water transfer. *a*, *b*, and *c* are
 564 calibrated parameters. *GW* is *groundwater*, *GW₀* represents water withdrawn from groundwater
 565 storage, *Dis* means groundwater discharge and is formulated as equation (17).

566 The calculation of *domestic* and *agricultural water demands* and consumptions is the same
 567 as in ANEMI3. *Industrial water demand* is dominated by the generation of electricity, which
 568 consists of both non-renewable sources (coal-fired and gas-fired thermal power) and renewable
 569 sources (hydropower and nuclear power). The *water withdrawal factor* and *water consumption* of
 570 thermal energy vary substantially among different cooling methods and their values for different
 571 fuel sources are obtained from Zhang et al. (2016) and shown in Table 2. Nuclear power plants in
 572 the Belt are located in coastal areas and rely on the withdrawal of only seawater, so the freshwater
 573 withdrawal and consumption factors of nuclear power are all set to zero. The calculation of
 574 *electricity water demand* takes the following form.

575
$$W_{ele} = Tech_{ele} \cdot \sum_{i=1}^4 E_{P_i} \cdot \sum_{j=1}^n WWF_{i,j} \cdot F_{i,j} \quad (18)$$

576 where *W_{ele}* is *electricity water demand*; *E_{P_i}*

577 *is electricity production* for energy source *i*; *WWF_i* is
 578 *water withdrawal factor* for energy source *i*; *F_{i,j}* is the fraction of cooling method *j* for energy
 579 source *i* and is externally prescribed; *Tech_{ele}* is technological change for withdrawals in *electricity*
 579 *production* and is also exogenously specified. *Industrial water demand* is calculated as,

580
$$W_{ind} = \frac{1}{R_{ele}} \cdot W_{ele} \quad (19)$$

581 where *W_{ind}* is *industrial water demand*; *R_{ele}* is the ratio of *electricity water demand* to *industrial*
 582 *water demand* and is set to 0.7 in this research.

583 Table 2 Water withdrawal and consumption factors for electricity production

Energy source <i>i</i>	Cooling method <i>j</i>	Water withdrawal factor (m ³ /MWh)	Water consumption factor (m ³ /MWh)
Coal	OT	98.54	0.393

	RC	2.466	1.972
	DRY	0.438	0.448
Gas	OT	34.07	0.379
	RC	2.902	2.114
Nuclear	OT (seawater)	178	1.514
Hydro		0	0

584 Note: OT=once through, RC=recirculating

585 In ANEMI_Yangtze, water demand is defined as the amount of water needed for the domestic,
586 industrial, and agricultural sectors. We calculate water consumption as the desired consumption
587 assuming that consumption and withdrawal can always be met, which means we do not simulate
588 the unsatisfied demand directly. Instead, we use *water stress* as a measure of water shortage. The
589 definitions and formulations of *water stress* are described in the following section.

590 In ANEMI3, water supply is incorporated as a new production sector within the energy-
591 economy sector. In ANEMI_Yangtze, we significantly simplified the development of water supply
592 by detaching it from the energy-economy sector. In other words, the water supply is developed
593 independently. We also exclude the effect of water pricing (through depletion and saturation) on
594 water supply development. In addition, we only consider three supply types: surface water,
595 groundwater, and wastewater reclamation. The production of water supplies is driven
596 economically by investing in *water supply capital* stocks for each source. The structure and
597 formulation of water supply development follow that of the energy capital development. Similarly,
598 the effect of *water stress* is introduced as an indicator for *water supply capital* investment and has
599 four definitions (a value bigger than 1 indicting water shortage). The *base water stress* WS_{base} is
600 represented as,

$$601 \quad WS_{base} = \frac{W_{dom} + W_{ind} + W_{agr}}{SW_{avai}} \quad (20)$$

602 where SW_{avai} is *available surface water*, which is the stable and reusable portion of the total
603 renewable streamflow..

604 The *water stress with groundwater and wastewater* WS_{gw+ww} is represented as,

$$605 \quad WS_{gw+ww} = \frac{W_{dom} + W_{ind} + W_{agr}}{SW_{avai} + r_{gw} \times GW + TRW} \quad (21)$$

606 where r_{gw} is *groundwater use ratio*, set to 0.01 based on the ratio of historical groundwater
607 withdrawals to total withdrawals; GW is *groundwater*; TRW is *treated returnable waters*.

608 The water stress with pollution effects $WS_{pollution}$ is represented as,

609
$$WS_{pollution} = \frac{W_{dom} + W_{ind} + W_{agr}}{SW_{avai} - f_{ww} \times UTRW}$$
 (22)

610 where f_{ww} is wastewater pollution factor, set to 8 (based on Shiklomanov (2000)); $UTRW$ is
611 untreated returnable waters.

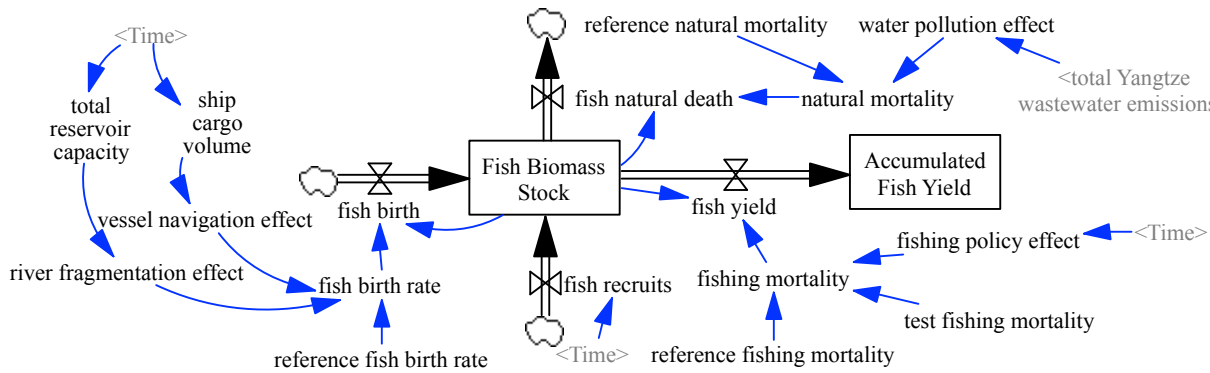
612 The water stress with water supply capacity WS_{supply} is represented as,

613
$$WS_{supply} = \frac{W_{dom} + W_{ind} + W_{agr}}{TWS}$$
 (23)

614 where TWS is total water supply capacity, which is the sum of surface water supply capacity,
615 groundwater supply capacity, and treated returnable waters.

616 **4.7 Fish**

617 The Fish Sector, which is an entirely new addition to the ANEMI_Yangtze model, is used to
618 simulate the dynamic of fish biomass stock over time. Figure 16 shows the stock and flow diagram
619 of the Fish Sector.



620

621 **Figure 16.** Stock and flow of the Fish Sector

622 The calculation of fish biomass stock is given as,

623
$$F = \int (f_b + f_r - f_a - f_y) dt$$
 (24)

624 where F is fish biomass stock, f_b is fish birth. f_r represents fish recruits, which is treated as an
625 exogenous variable. f_a is natural fish death, f_y is fish yield.

626 Fish catch data come from Zhang et al. (2020). Major parameters in the Fish Sector are given
627 in Table 3.

628 Table 3 Major parameters and their corresponding values in the Fish Sector

Variable	Value	Unit	Source
reference natural mortality	0.075	dmnl	Gilbert et al. (2000)

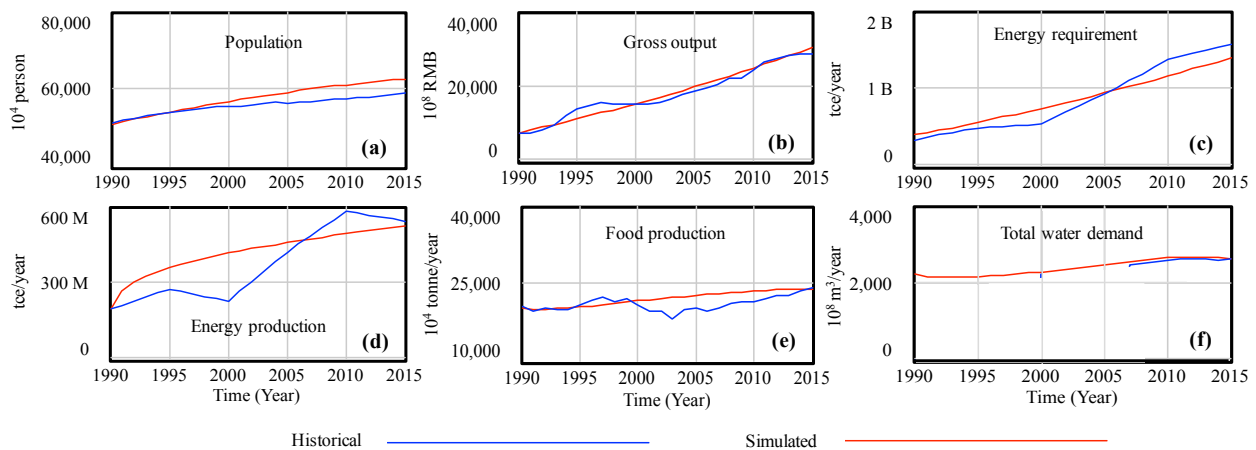
reference fishing mortality	0.7949	dmnl	Chen et al. (2009)
reference fish birth rate	0.826	dmnl	Zhang et al. (2020)

629 Note: for *reference fishing mortality* the value of 0.7949 is calculated based on Chen et al.
630 (2009) by averaging the exploitation coefficients of 10 economically fish species (fishing mortality
631 = 0.761, 0.706, 0.803, 0.829, 0.898, 0.876, 0.846, 0.774, 0.765 and 0.691). For *reference fish birth*
632 *rate* the value of 0.826 is calculated based on Zhang et al. (2020) by averaging fish growth rates
633 in the middle Yangtze reach, Dongting lake, and Poyang lake.

634 5. Model validation and application

635 5.1 Model validation and sensitivity analysis

636 The ANEMI_Yangtze model was validated by comparing model simulated results with
637 available historical data for 1990-2015. The results shown in Figure 17 indicate that the model can
638 reproduce the system behaviour very well for *population*, *gross economic output*, and *water*
639 *demand* (Figure 17(a, b, and f)). The model can capture the general behaviour patterns for *energy*
640 *requirement*, *energy production*, and *food production* (Figure 17(c-e)). The fluctuations of
641 historical *food production* are mainly attributed to the flood and drought disasters, which are not
642 currently captured by the model. The discrepancies between historical and simulated *energy*
643 *requirement* and *energy production* are partly due to the previous energy policies acting on the
644 energy system that the model doesn't consider. For example, in China, overcapacity in coal
645 production gradually appeared after the mid-1990s, and this situation worsened after the outbreak
646 of the 1997 Asian financial crisis. To alleviate the overcapacity crisis, the governments at all levels
647 issued series of policies to reduce production, seen as the production drop around year 2000 (Figure
648 17(d)).



649

650 **Figure 17.** Comparison of simulated and historical system behaviour

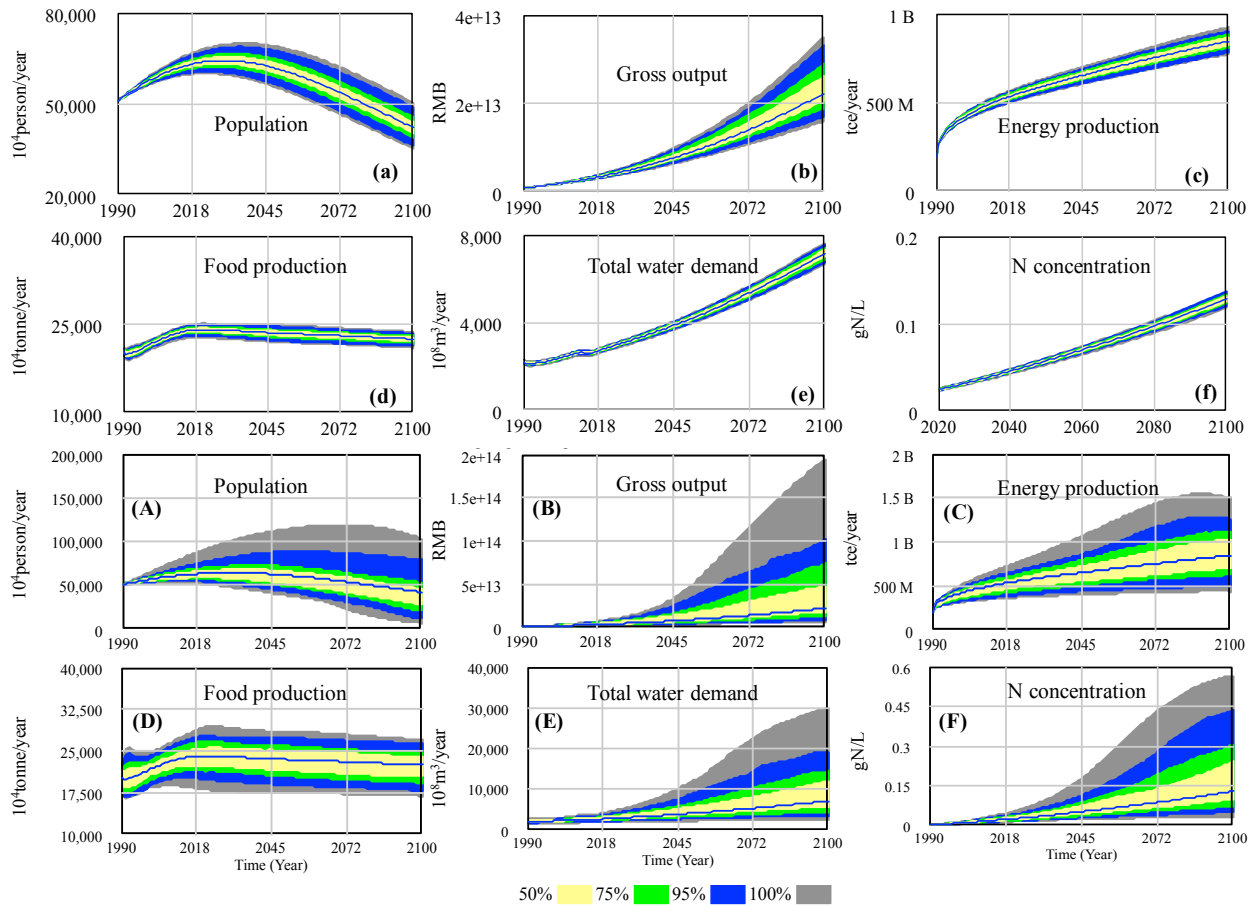
651 Sensitivity analysis aims to build confidence in the model's ability to generate robust system
652 behaviour by applying Monte Carlo simulation. The parameters used for sensitivity tests (shown
653 in Table 4) are chosen due to uncertainty in their values. The selected parameters are varied by -
654 10% ~ +10% (mild variation scenario) and -50% ~ +50% (extreme variation scenario) to determine
655 whether the main state variables will exhibit alternative behaviour. Triangular probability
656 distribution is used. The highest point of probability in the triangle is assigned to the baseline value
657 of these parameters, where the outer limits are defined by the minimum and maximum percent
658 changes of the value.

659 The sensitivity simulations are performed by considering all the possible parameter change
660 combinations together, and the results are shown in Figure 18. The lowercase letters show the
661 results for the mild variation scenario and the capital letters for the extreme variation scenario. As
662 can be seen, the range of the projected variables becomes smaller with the decreasing of the
663 confidence level. For each of the examined variables shown in Figure 18 (a-f), the behaviour
664 modes remain the same within the range of the parameters tested when the variation is mild (-10%
665 ~ +10%). When the variation is extreme (-50% ~ +50%), the range in the trajectory of the state
666 variables is larger, however, the behaviour of each variable still remains the same (Figure 18 (A-
667 F)). The lack of changes in behaviour modes while testing model sensitivity is desirable, indicating
668 the model is robust.

Table 4 Parameters used for sensitivity tests of main state variables in the model

State variable	Parameters	Baseline value	Unit
Population	normal life expectancy	52.5	year
	female ratio	0.5	dmnl
	reproductive lifetime	35	year
Gross output	value share of labor	0.6	dmnl
	capital energy substitution elasticity	0.75	dmnl
	capital lifetime	40	year
Food production	per capita food consumption	400	kg/year/person
	normal average life of land	6000	year
	inherent land fertility	6300	kg/hectare/ year
Energy production	energy resource elasticity [coal, oil, gas, hydro, nuclear, new]	0.625, 0.657, 0.657, 0.303, 0.303, 0.527	dmnl
	energy capital lifetime [coal, oil, gas, hydro, nuclear, new]	15, 15, 15, 30, 30, 20	year
	reference energy consumption per unit GDP	6	tce/10000rmb
Water demand	reference water withdrawal factor [coalOT, coalRC, coalDRY, gasOT, gasRC, hydro, nuclearOT]	98.54, 2.47, 0.44, 34.07, 2.90, 0, 0	m ³ /MWh
	initial water intake	4000	m ³ /hectare/ year
Nitrogen concentration	N leaching coefficient of agricultural runoff	18.65	kg/hectare/year
	N concentration of domestic wastewater	60	g/L
	N concentration of industrial wastewater	60	g/L

670 Note: The values of N concentration of domestic/industrial wastewater are from Henze and Comeau (2008), and the
671 value of N leaching coefficient of agricultural runoff is obtained from FAO
672 (<http://www.fao.org/3/w2598e/w2598e06.htm>, last accessed Sep 20, 2021). Energy resource elasticities are from
673 ANEMI (Breach and Simonovic, 2020).



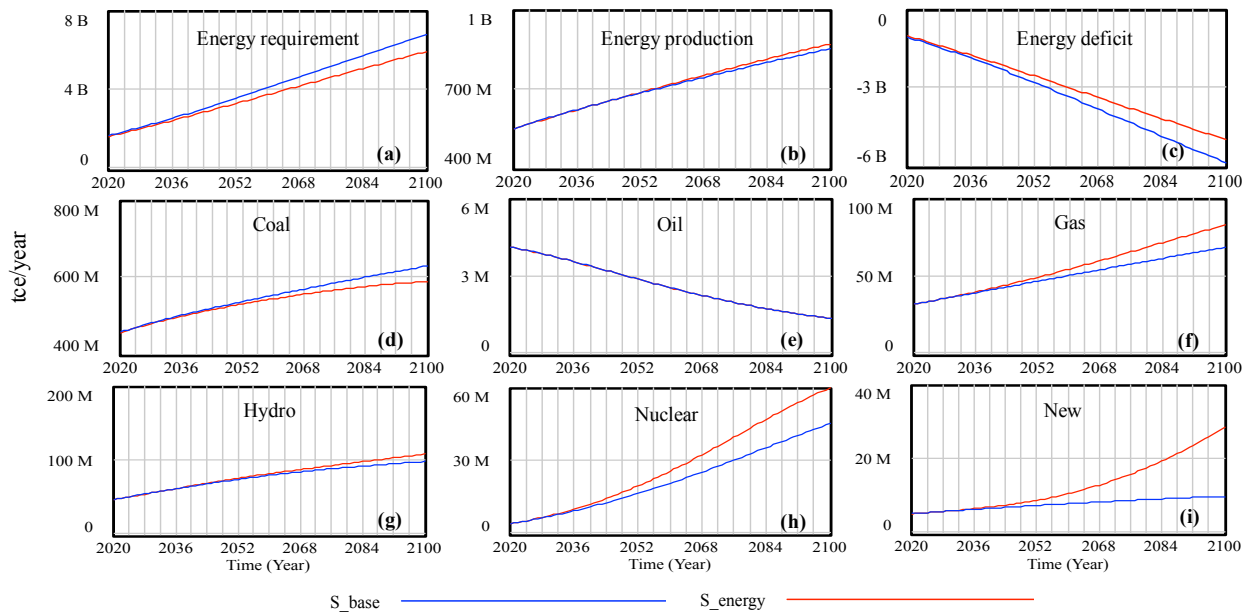
674
675 **Figure 18.** Sensitivity of the selected state variables

676 **5.2 Model application**

677 To test the capabilities of ANEMI_Yangtze, this section focuses on the applications of the
 678 model system for the baseline S_base scenario and S_energy scenario. Under the S_base scenario,
 679 all the policies remain at their 2015 values during the simulation. Specifically, the one-child policy
 680 remains unchanged for the *Population Sector*. The intensity of water withdrawals/consumptions
 681 in industry and agriculture for the *Water Sector*, the *energy shares* among different energy sources
 682 for the *Energy Sector*, and the *fishing mortality* for the *Fish Sector* shall all remain their 2015
 683 values respectively. The N/P removal efficiency in the *Nutrient Sector* is 0. The exogenous inputs
 684 of precipitation and temperature take their historical average annual values. Under the S_energy
 685 scenario, the *energy share* of coal decreases linearly from around 60% (the 2015 share) to 30%,
 686 and the share of renewable energy (hydropower, nuclear, and new energy sources) increases from
 687 15% to 30% by 2100. The simulation results are shown in Figures 19-20.

688 As the share of gas and renewable energy sources increases in the S_energy scenario, the
 689 demand for those energy sources grows, placing more pressure on their production. The *energy*

690 *production pressure effect* acts as a positive factor on *energy capital investment*. Therefore more
 691 money is poured into producing energy from gas and renewables sources. As more *energy capital*
 692 is mobilized for gas and renewable energy development, the improvement in *energy technology*
 693 advances correspondingly, leading to a decrease in *energy consumption intensity per unit GDP*,
 694 thus lowering the *energy demand* compared to the base run (see Figure 19(a)). Besides, the
 695 combined effects of growing *energy capital investment* and *energy technology* advancement lead
 696 to a substantial increase in effective production effort, resulting in increases in gas production,
 697 hydropower, nuclear power, and new energy sources, as seen in Figures 19 (f-i). The production
 698 of coal is expected to decrease compared to the base run, along with its decrease in energy share
 699 (Figure 19(d)). As the energy share of oil remains the same value as in the S_base scenario, its
 700 production also remains at the base run level (Figure 19(e)). Those combined effects of the increase
 701 in gas and renewable energy production and decrease in coal production result in a slight increase
 702 in the total production of energy compared to the base run result (Figure 19(b)).

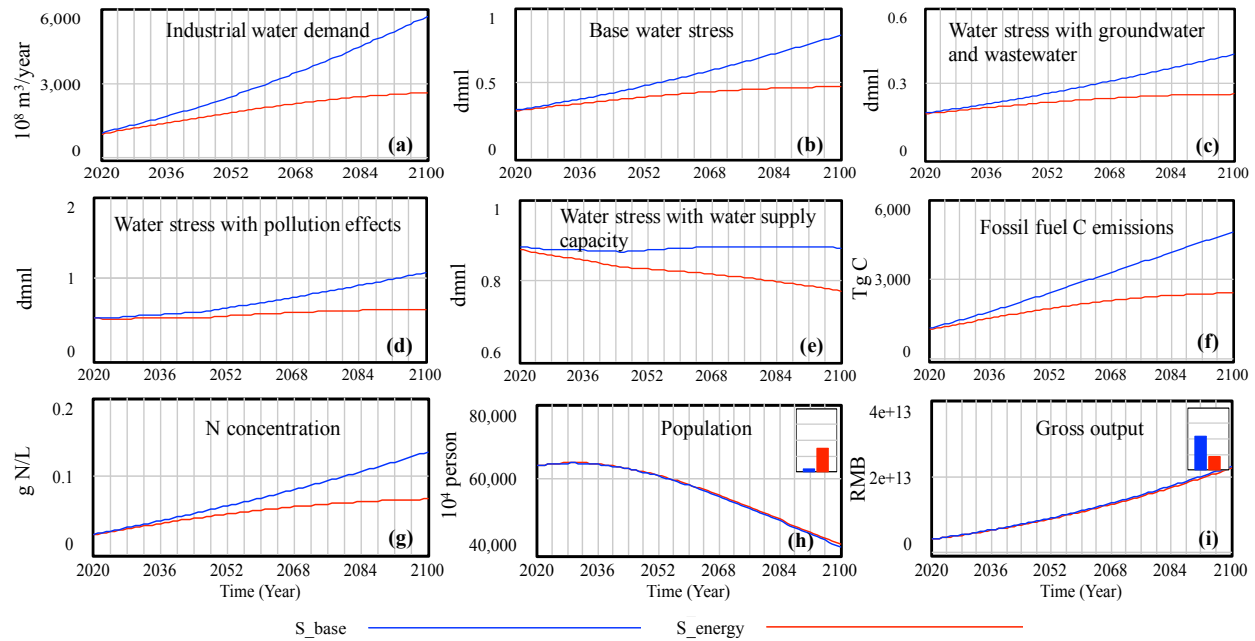


703
 704 **Figure 19.** Effects of energy policy on energy system

705 The changing patterns of *energy consumption* have significant impacts on water and carbon
 706 systems. In the S_base run, the coal-fired thermal power plants dominate the *water demand* in the
 707 industrial sector. In this S_energy scenario, coal's share decreases from 60% to 30%, and the value
 708 share of renewable energy (hydropower, nuclear, and new energy sources) increases from 15% to
 709 30% by the end of the simulation. The nuclear power plants in the Belt are usually located near
 710 the East China sea. The cooling water comes directly from the seawater, therefore not increasing

711 freshwater withdrawal. The hydropower plants and the new energy sources (wind and solar power)
712 do not consume any water. This leads to a considerable drop in industrial water demand, as can be
713 seen in Figure 20(a). In the S_base run, the industrial water demand by 2100 approaches 600 billion
714 m³, while in the S_energy scenario, the value halves and lies below 300 billion. As the industrial
715 sector replaces the agricultural sector, it becomes the most significant water consumer after 2030.
716 Under all definitions, the *water stress* reduces substantially, with all values lying below the critical
717 value of 1 (Figures 20(b-e)). A decrease in industrial water demand and withdrawal also reduces
718 industrial wastewater in accordance and lowers the level of nutrient concentration. The
719 concentration level of nitrogen is shown in Figure 20(g); the results of phosphorus concentration,
720 which share the same behaviour as the nitrogen, are not shown in the figure. By the end of the
721 simulation, the carbon emissions fall from 4,800 Tg in the S_base run to about 2,500 Tg in the
722 S_energy scenario as a result of cutting the coal consumption by half.

723 The changing energy consumption pattern also has some impacts on population growth and
724 economic development. A slight increase in population is observed under S_energy scenario (see
725 Figure 20(h)) when compared to the base run. This is due to the reduction of nitrogen and
726 phosphorus concentration levels, which improve *life expectancy* through a variable - *lifetime*
727 *multiplier from pollution*. As for the economy, even though there is a slightly higher supply of
728 *labour force* resulting from an increase in population, the Belt's *gross output* in the S_energy
729 scenario is a little bit lower than in the S_base output (Figure 20(i)). This is due to the reduced
730 *energy requirement* as seen in Figure 20(a) and discussed in the previous section. A decrease in
731 *energy requirement* decreases the *capital-energy aggregate*, which then decreases the *operating*
732 *capital*, leading to the decline in economic output. In this application, the effect of decreasing
733 *operating capital* on economic output outpaces the effect of boosting the *labour force* on economic
734 output.



735
736 **Figure 20.** Effects of energy policy on the Belt system

737 **6. Conclusion and discussion**

738 To address the specific challenges facing Yangtze Economic Belt’s sustainable development,
739 ANEMI_Yangtze, which consists of the *Population, Economy, Land, Food, Energy, Water,*
740 *Carbon, Nutrients,* and *Fish Sectors* was developed based on the feedback-based integrated global
741 assessment model ANEMI3. This paper focuses on: (i) the identification of the cross-sectoral
742 interactions and feedbacks involved in shaping the Belt’s system behaviour over time; (ii) the
743 identification of the feedbacks within each sector that drive the state variables in that sector; and
744 (iii) the description of a new *Fish Sector* and modifications in the *Population, Food, Energy,* and
745 *Water Sectors,* including the underlying theoretical basis for model equations. The model was
746 validated by comparing simulated results with available historical data. Sensitivity analysis was
747 conducted by varying the parameters with high degree of uncertainty by -10% ~ +10% (mild
748 variation scenario) and -50% ~ +50% (extreme variation scenario). Results demonstrate the
749 model’s robustness in modeling system behavioural.

750 In the application section, the impacts of shifting energy consumption patterns was
751 investigated. As the Belt gradually shifts its *energy consumption* from coal to natural gas and
752 renewable energy sources, the total *energy production* increases slightly. In contrast, the total
753 *aggregated energy requirement* declines significantly due to the effects of *energy technology*
754 advances. It is also found that the industrial *water demand* and the fossil fuel carbon emissions are

755 greatly reduced, leading to a decrease in nutrient concentration levels and an increase in population.
756 The Belt's *gross output* in the S_{energy} scenario is lower than the base output as the effect of
757 decreasing *operating capital*, which is caused by a decrease in total *aggregated energy*
758 *requirement*, outpaces the effect of boosting the *labour force*. These findings enhance our
759 integrated understanding of the dynamic behaviour of socio-economic development, natural
760 resources depletion, and environmental impacts in the Belt. More in-depth model simulation
761 analyses are needed to better understand the influences, responses, and feedbacks generic dynamic
762 behavior of the Belt. The development of policy scenarios and the analyses of associated outcomes
763 are presented in another paper (Jiang et al., 2021).

764 This paper focuses on presenting the feedback that drive the Belt's dynamic system behaviour
765 based on the authors' current knowledge and understanding. It should, however, be kept in mind
766 that some of the feedbacks might be missing due to the data necessary to describe these feedbacks
767 are currently not available. For example, in China, fish plays an important dietary role and
768 therefore, there should exist feedback connecting the *fish yield* and *food production*. Persistent
769 pollution, a clear consequence of China's rapid economic development, should also be included.
770 There are thus constant drivers to extend and improve the model framework as more data becomes
771 available or as the state-of-the-knowledge progresses, or as scientific questions become more
772 complex.

773
774 *Code availability.* The version of ANEMI_Yangtze described in this paper is archived on Zenodo
775 (<http://doi.org/10.5281/zenodo.4764138>). The code can be opened using the Vensim software to
776 view the model structure. A free Vensim PLE licence can be obtained from <https://vensim.com>,
777 which can be used to view the stock and flow diagram that makes up the model structure. Due to
778 the advanced features used in the ANEMI_Yangtze model, a Vensim DSS license is required to
779 run the model.

780 *Author contribution.* **Haiyan Jiang:** Methodology, Investigation, Validation, Writing - original
781 draft. **Slobodan P. Simonovic:** Conceptualization, Software, Writing - review & editing,
782 Supervision. **Zhongbo Yu:** Funding acquisition, Writing - review & editing.

783

784 *Competing interests.* The authors declare that they have no conflict of interest.

785 *Acknowledgements.* This work was supported by the Fundamental Research Funds for the Central
786 Universities (Grant No. B200202035); the Belt and Road Special Foundation of the State Key
787 Laboratory of Hydrology-Water Resources and Hydraulic Engineering (Grant No. 2020490111);
788 the National Key R&D Program of China (Grant No. 2016YFC0402710); National Natural
789 Science Foundation of China (Grant No. 51539003, 41761134090, 51709074); the Special Fund
790 of State Key Laboratory of Hydrology-Water Resources and Hydraulic Engineering (Grant No.
791 20195025612, 20195018812, 520004412). The authors are thankful for the financial support of
792 the presented research provided to the second author by the Natural Sciences Research Council of
793 Canada under the discovery grant program.

794 **References**

- 795 Akhtar, M. K., Simonovic, S. P., Wibe, J., and MacGee, J.: Future realities of climate change
796 impacts: An integrated assessment study of Canada, *Int. J. Global Warm.*, 17, 59-88,
797 <https://doi.org/10.1504/IJGW.2019.10017598>, 2019.
- 798 Akhtar, M. K., Wibe, J., Simonovic, S. P., and MacGee, J.: Integrated assessment model of
799 society-biosphere-climate-economy-energy system, *Environ. Modell. Softw.*, 49, 1-21.
800 <http://doi.org/10.1016/j.envsoft.2013.07.006>, 2013.
- 801 Allen, C., Metternicht, G., and Wiedmann, T.: National pathways to the Sustainable
802 Development Goals (SDGs): A comparative review of scenario modelling tools, *Environ.*
803 *Sci. Policy*, 66, 199-207, <https://doi.org/10.1016/j.envsci.2016.09.008>, 2016.
- 804 Bauer, N., Baumstark, L., and Leimbach, M.: The REMIND-R model: The role of renewables
805 in the low-carbon transformation — first-best vs. second-best worlds, *Climatic Change*,
806 114, 145-168, doi: 10.1007/s10584-011-0129-2, 2012.
- 807 Bazilian, M., Rogner, H., Howells, M., Hermann, S., Arent, D., Gielen, D., Steduto, P.,
808 Mueller, A., Komor, P., Tol, R. S. and Yumkella, K. K.: Considering the energy, water and
809 food nexus: Towards an integrated modelling approach, *Energ. Policy*, 39, 7896-7906,
810 <https://doi.org/10.1016/j.enpol.2011.09.039>, 2011.
- 811 Beek, L. V., Vuuren, D., Hajer, M., et al.: Anticipating futures through models: the rise of
812 Integrated Assessment Modelling in the climate science-policy interface since 1970,
813 *Global Environ. Chang.*, 65, 102191, <https://doi.org/10.1016/j.gloenvcha.2020.102191>,
814 2020.

815 Breach, P.: Water Supply Capacity Development in the Context of Global Change, Electronic
816 Thesis and Dissertation Repository, 6930. <https://ir.lib.uwo.ca/etd/6930>, 2020.

817 Breach, P. A., and Simonovic, S. P.: ANEMI: A tool for global change analysis, Plos One, 16,
818 0251489, <https://doi.org/10.1371/journal.pone.0251489>, 2021.

819 Calvin K., and Bond-Lamberty, B: Integrated human-earth system modeling — state of the
820 science and future directions, Environ. Res. Lett., 13, 063006,
821 <https://doi.org/10.1088/1748-9326/aac642>, 2018.

822 Calvin, K., Patel, P., Clarke, L., Asrar, G., Bond-Lamberty, B., Cui, R.Y., Vittorio, A.D.,
823 Dorheim, K., Edmonds, J., Hartin, C., and Hejazi, M.: GCAM v5.1: Representing the
824 linkages between energy, water, land, climate, and economic systems, Geosci. Model Dev.,
825 12, 677-698, <https://doi.org/10.5194/gmd-12-677-2019>, 2019.

826 Cao, L., Zhang, Y., and Shi, Y.: Climate change effect on hydrological processes over the
827 Yangtze River basin, Quatern. Int., 244, 202-210,
828 <https://doi.org/10.1016/j.quaint.2011.01.004>, 2011.

829 Chen, D., Xiong, F., Wang, K., and Chang, Y.: Status of research on Yangtze fish biology and
830 fisheries, Environ. Biol. Fish., 85, 337-357, <https://doi.org/10.1007/s10641-009-9517-0>,
831 2009.

832 Clark, W.A.V., Yi, D., and Zhang, X.: Do house prices affect fertility behavior in China? An
833 empirical examination, Int. Regional Sci. Rev., 43(5), 423-449,
834 <https://doi.org/10.1177/0160017620922885>, 2020.

835 Clayton, T., and Radcliffe, N.: Sustainability: A systems approach, Routledge, 2018.

836 Davies, E. G. R, and Simonovic, S. P.: ANEMI: A new model for integrated assessment of
837 global change, Interdisciplinary Environmental Review, 11, 127-161,
838 <https://doi.org/10.1504/IER.2010.037903>, 2010.

839 Davies, E. G. R, and Simonovic, S. P.: Global water resources modeling with an integrated
840 model of the social-economic-environmental system, Adv. Water Resour., 34, 684-700,
841 <https://doi.org/10.1016/j.advwatres.2011.02.010>, 2011.

842 Department of Energy at National Bureau of Statistics (DENBS): China Energy Statistical
843 Yearbook in 2015. China Statistics Press, Beijing, 2016 (in Chinese).

844 Dermody, B. J., Sivapalan, M., Stehfest, E., Vuuren, D., and Dekker, S. C.: A framework
845 for modelling the complexities of food and water security under globalisation, *Earth Syst.*
846 *Dynam.*, 9, 103-118, <https://doi.org/10.5194/esd-2017-38>, 2018.

847 Dettling, L.J., Kearney, M.S.: House prices and birth rates: The impact of the real estate market
848 on the decision to have a baby, *J. Public Econ.*, (1), 82-100,
849 <https://doi.org/10.1016/j.jpubeco.2013.09.009>, 2014.

850 Dinar, A., Tieu, A., and Huynh, H.: Water scarcity impacts on global food production, *Glob.*
851 *Food Secur.*, 23(3), 212-226, <https://doi.org/10.1016/j.gfs.2019.07.007>, 2019.

852 D'Odorico, P., Davis, K. F., Rosa, L., Carr, J. A., Chiarelli, D., Dell'Angelo, J., Gephart, J.,
853 MacDonald, G. K., Seekell, D. A., Suweis, S., and Rulli, M. C.: The global food-energy-
854 water nexus, *Rev. Geophys.*, 56, 456-531, <https://doi.org/10.1029/2017RG000591>, 2018.

855 European Commission: Energy in Europe, European energy to 2020: A scenario approach.
856 Belgium: Directorate general for energy, 1996.

857 Fang, Y., Zhang, W., Cao, J., and Zhu, L.: Analysis on the current situation and development
858 trend of energy resources in China, *Conservation and Utilization of Mineral Resources*, 4,
859 34-42, 2018, (in Chinese).

860 Fiddaman, T. S.: Feedback complexity in integrated climate-economy models, Department of
861 Operations Management and System Dynamics, Massachusetts Institute of Technology,
862 Cambridge, Massachusetts, 1997.

863 Fisher-Vanden, K., and Weyant, J.: The evolution of integrated assessment: Developing the
864 next generation of use-inspired integrated assessment tools, *Annu. Review Resour. Econ.*,
865 12, 471-487, <https://doi-org/10.1146/annurev-resource-110119-030314>, 2020.

866 Forrester, J. W.: *Industrial dynamics*. Cambridge, MA: Massachusetts Institute of Technology
867 Press, 1961.

868 Fu, B.: Promoting geography for sustainability, *Geography and Sustainability*, 1(1), 1-7,
869 <https://doi.org/10.1016/j.geosus.2020.02.003>, 2020.

870 Giorgi, F., Im, E.S., and Coppola, E., et al.: Higher hydroclimatic intensity with global
871 warming, *J. Climate*, 24(20), 5309-5324, <https://doi.org/10.1175/2011JCLI3979.1>, 2011.

872 Gilbert, D. J., McKenzie, J. R., Davies, N. M., and Field, K. D.: Assessment of the SNA 1
873 stocks for the 1999-2000 fishing year. *New Zealand Fisheries Assessment Report*, 38, 52,
874 2000.

875 Goudriaan, J., and Ketner, P.: A simulation study for the global carbon cycle, including man's
876 impact on the biosphere, *Climatic Change*, 6(2), 167-192, 1984.

877 Gu, H., Yu, Z., Wang, G., Wang, J., Ju, Q., Yang, C., and Fan, C.: Impact of climate change
878 on hydrological extremes in the Yangtze river basin, China, *Stoch. Env. Res. Risk A.*, 29,
879 693-707, <https://doi.org/10.1007/s00477-014-0957-5>, 2015.

880 Henze. M., and Comeau, Y.: Wastewater Characterization. In: *Biological Wastewater*
881 *Treatment: Principles Modelling and Design*. IWA Publishing, London, UK, 33-52, 2008.

882 Hertwich, E.G., Gibon, T., Bouman, E.A., et al.: Integrated life-cycle assessment of electricity-
883 supply scenarios confirms global environmental benefit of low-carbon technologies, P.
884 *Natl. Acad. Sci. USA*, 112, 6277-6282, <https://doi.org/10.1073/pnas.1312753111>, 2015.

885 Holman, I. P., Rounsevell, M. D. A., Cojocaru, G., Shackley, S., McLachlan, C., Audsley, E.,
886 Berry, P. M., Fontaine, C., Harrison, P. A., Henriques, C., and Mokrech, M.: The concepts
887 and development of a participatory regional integrated assessment tool, *Climatic Change*,
888 90, 5-30, <https://doi.org/10.1007/s10584-008-9453-6>, 2008.

889 Hopwood, B., Mellor, M., and O'Brien, G.: Sustainable development: Mapping different
890 approaches, *Sustainable Development*, 13, 38-52, <https://doi.org/10.1002/sd.244>, 2005.

891 Hui, E., Xian, Z., and Jiang, H.: Housing price, elderly dependency and fertility behaviour,
892 *Habitat Int.*, 36(2), 304-311, <https://doi.org/10.1016/j.habitatint.2011.10.006>, 2012.

893 Jeon, S., Roh, M., Oh, J., and Kim, S.: Development of an integrated assessment model at
894 provincial level: GCAM-Korea, *Energies*, 13, 2565, <https://doi.org/10.3390/en13102565>,
895 2020.

896 Jia, B., Zhou, J., Zhang, Y., and et al.: System dynamics model for the coevolution of coupled
897 water supply - power generation - environment systems : Upper Yangtze river Basin ,
898 China, *J. Hydrol.*, 593, 125892, <https://doi.org/10.1016/j.jhydrol.2020.125892>, 2021.

899 Jiang, H., and Simonovic, S. P.: ANEMI_Yangtze - A regional integrated assessment model
900 for the Yangtze Economic Belt in China. Water Resources Research Report no. 110,
901 Facility for Intelligent Decision Support, Department of Civil and Environmental
902 Engineering, London, Ontario, Canada, 75 pages. ISBN: (print) 978-0-7714-3155-5;
903 (online) 978-0-7714-3156-2, 2021.
904 <https://www.eng.uwo.ca/research/iclr/fids/publications/products/111.pdf>.

905 Jiang, H. , Simonovic, S. P., Yu, Z. , and Wang, W.: System dynamics simulation model for
 906 flood management of the three gorges reservoir, *J. Water Res. Plan. Man.*, 146, 05020009,
 907 [https://doi.org/10.1061/\(ASCE\)WR.1943-5452.0001216](https://doi.org/10.1061/(ASCE)WR.1943-5452.0001216), 2020.

908 Jiang, H. , Simonovic, S. P., Yu, Z. , and Wang, W.: What are the main challenges facing the
 909 sustainable development of China's Yangtze Economic Belt in the future? An integrated
 910 view, *Environ. Res. Commun.*, 3, 115005, <https://doi.org/10.1088/2515-7620/ac35bd>,
 911 2021.

912 Ju, H., Liu, Q., Li, Y., et al.: Multi-stakeholder efforts to adapt to climate change in China's
 913 agricultural sector, *Sustainability*, 12, <https://doi.org/10.3390/su12198076>, 2020.

914 Klein, J. T., Grossenbacher-Mansuy, W., Häberli, R., Bill, A., Scholz, R. W., and Welti, M.
 915 eds.: *Transdisciplinarity: Joint problem solving among science, technology, and society:
 916 An effective way for managing complexity*, Springer Science & Business Media, 2001.

917 Kong, L., Zheng, H., Rao, E., Xiao, Y., Ouyang, Z., and Li, C.: Evaluating indirect and direct
 918 effects of eco-restoration policy on soil conservation service in Yangtze River Basin, *Sci.
 919 Total Environ.*, 631, 887-894, <https://doi.org/10.1016/j.scitotenv.2018.03.117>, 2018.

920 Kriegler, E., Bauer, N., Popp, A., Humpenöder, F., Leimbach, M., Strefler, J., Baumstark, L.,
 921 Bodirsky, B. L., Hilaire, J., Klein, D., Mouratiadou, I., Weindl, I., Bertram, C., Dietrich,
 922 J.-P., Luderer, G., Pehl, M., Pietzcker, R., Piontek, F., Lotze-Campen, H., Biewald, A.,
 923 Bonsch, M., Giannousakis, A., Kreidenweis, U., Müller, C., Rolinski, S., Schultes, A.,
 924 Schwanitz, J., Stevanovic, M., Calvin, K., Emmerling, J., Fujimori, S., and Edenhofer, O.:
 925 Fossil-fueled development (SSP5): An energy and resource intensive scenario for the 21st
 926 century, *Global Environ. Chang.*, 42, 297-315,
 927 <https://doi.org/10.1016/j.gloenvcha.2016.05.015>, 2017.

928 Lee, E.S.: *A Theory of Migration*. *Demography*, 3(1), 47-57, 1966.

929 Lei, G., Fu, C., Zhang, L., et al.: The changes in population floating and their influencing
 930 factors in China based on the sixth census, *Northwest Population Journal*, 34(05), 1-8,
 931 <https://doi.org/10.15884/j.cnki.issn.1007-0672.2013.05.017>, 2013. (in Chinese)

932 Li, J., Glibert, P.M., Zhou, M., Lu, S., and Lu, D.: Relationships between nitrogen and
 933 phosphorus forms and ratios and the development of dinoflagellate blooms in the East
 934 China Sea, *Mar. Ecol. Prog. Ser.*, 383, 11-26, <https://doi.org/10.3354/meps07975>, 2009.

935 Li, Y., Acharya, K., and Yu, Z.: Modeling impacts of Yangtze River water transfer on water
936 ages in Lake Taihu, China, *Ecol. Eng.*, 37, 325-334,
937 <https://doi.org/10.1016/j.ecoleng.2010.11.024>, 2011.

938 Li, Z., He, Y., Pu, T., Jia, W., He, X., Pang, H., Zhang, N., Liu, Q., Wang, Sh., Zhu, G., Wang,
939 Sh., Chang, L., Du, J., and Xin, H.: Changes of climate, glaciers and runoff in China's
940 monsoonal temperate glacier region during the last several decades, *Quatern. Int.*, 218, 13-
941 28, <https://doi.org/10.1016/j.quaint.2009.05.010>, 2010.

942 Liu, L., and Ding, Y.: Hydraulic resources and hydropower planning in the Yangtze River
943 Basin, *Yangtze River*, 44, 69-71, 2013, (in Chinese).

944 Liu J.G., Dietz, T., Carpenter, S.R., et al.: Complexity of coupled human and natural systems,
945 *Science*, 317 (5844), 1513-1516, <https://doi.org/10.1126/science.1144004>, 2007.

946 Liu, Y., Wang, S., and Chen, B.: Regional water-energy-food nexus in China based on
947 multiregional input-output analysis, *Energy Procedia*, 142, 3108-3114,
948 <https://doi.org/10.1016/j.egypro.2017.12.452>, 2017.

949 Loulou, R.: ETSAP-TIAM: The TIMES integrated assessment model. Part II: Mathematical
950 formulation, *Comput. Manag. Sci.*, 5, 41-66, <https://doi.org/10.1007/s10287-007-0045-0>,
951 2007.

952 Ma, L., and Yu, Z.: Influencing factors of Chinese average life expectancy, *Economic*
953 *Research Guide*, (01), 161-162, 2009.

954 Mackenzie, F.T., Ver, L.M., Sabine, C., and Lane, M.: C, N, P, S global biogeochemical cycles
955 and modeling of global change, *Interactions of C, N, P and S Biogeochemical Cycles and*
956 *Global Change*, Springer, Verlag, 1-61, 1993.

957 Matsuoka, Y., Kainuma, M., and Morita, T.: Scenario analysis of global warming using the
958 Asian-Pacific integrated model (AIM), *Energ. Policy*, 23, 357-371, 10.1016/0301-
959 4215(95), 90160-9, 1995.

960 Meadows, D.L., Behrens, W.W., Meadows, D.H., et al.: *Dynamics of Growth in a Finite World*.
961 Wright-Allen Press, Inc. Cambridge, Massachusetts, 1974.

962 Messner, S., and Strubegger, M.: *User's Guide for MESSAGE III*, Working Paper WP-95-069,
963 International Institute for Applied Systems Analysis (IIASA), Laxenburg, Austria, 1995,
964 p. 164.

965 Messner, S., and Schrattenholzer, L.: MESSAGE-MACRO: linking an energy supply model
966 with a macroeconomic module and solving it iteratively, *Energy*, 25, 267-282,
967 [https://doi.org/10.1016/S0360-5442\(99\)00063-8](https://doi.org/10.1016/S0360-5442(99)00063-8), 2000.

968 MIIT: Innovation-driven industrial transformation and upgrading plan for the Yangtze River
969 Economic Belt. Ministry of Industry and Information Technology of the People's Republic
970 of China, 2016.

971 National Development and Reform Commission (NDRC): Development and planning outline
972 of the Yangtze River Economic Belt officially released, 2016.
973 <http://www.sc.gov.cn/10462/10758/10760/10765/2016/9/20/10396398.shtml>

974 Niva, V., Cai, J., Taka, M., Kummu, M., Varis, O.: China's sustainable water-energy-food
975 nexus by 2030: Impacts of urbanization on sectoral water demand, *J. Clean. Prod.*, 251,
976 119755, <https://doi.org/10.1016/j.jclepro.2019.119755>, 2020.

977 Nordhaus, W.D., and Boyer, J.: *Warming the world: Economic models of global warming*.
978 The MIT Press, Cambridge, Massachusetts, U.S.A., 2000.

979 Pautrel, X.: Pollution and life expectancy: How environmental policy can promote growth,
980 *Ecol. Econ.*, 68(4), 1040-1051, <https://doi.org/10.1016/j.ecolecon.2008.07.011>, 2009.

981 Pedercini, M., Arquitt, S., Collste, D., and Herren, H.: Harvesting synergy from sustainable
982 development goal interactions, *P. Natl. Acad. Sci. USA*, 46, 23021-23028,
983 <https://doi.org/10.1073/pnas.1817276116>, 2019.

984 Qin, B. Q., Wang, X. D., Tang, X. M., Feng, S., and Zhang, Y. L.: Drinking water crisis caused
985 by eutrophication and cyanobacterial bloom in Lake Taihu: cause and measurement,
986 *Advances in Earth Science*, 22, 896-906, <https://doi.org/10.3321/j.issn:1001-8166.2007.09.003>, 2007. (in Chinese)

987

988 Qu, W.S., Barney, G., Symalla, D., and Martin, L.: Threshold 21: national sustainable
989 development model, *Integrated Global Models of Sustainable Development*, 2, 78-87, 1995.

990 Qu, W., Shi, W., Zhang, J., and Liu, T.: T21 China 2050: A Tool for national sustainable
991 development planning, *Geography and Sustainability*, 1(1), 33-46,
992 <https://doi.org/10.1016/j.geosus.2020.03.004>, 2020.

993 Shen, J.: Increasing internal migration in China from 1985 to 2005: Institutional versus
994 economic drivers, *Habitat Int.*, 39, 1-7, <https://doi.org/10.1016/j.habitatint.2012.10.004>,
995 2013.

996 Shi, W., Ou, Y., Smith, S. J., Ledna, C. M., Nolte, C. G., and Loughlin, D. H.: Projecting state-
997 level air pollutant emissions using an integrated assessment model: GCAM-USA, *Appl.*
998 *Energ.*, 208, 511-521, <https://doi.org/10.1016/j.apenergy.2017.09.122>, 2017.

999 Shiklomanov, I. A.: Appraisal and assessment of world water resources, *Water Int.*, 25, 11-32,
1000 <https://doi.org/10.1080/02508060008686794>, 2000.

1001 Simonovic, S. P.: Global water dynamics: Issues for the 21st century, *Journal of Water Science*
1002 *and Technology*, 45, 53-64, <https://doi.org/10.2166/wst.2002.0143>, 2002.

1003 Simonovic, S. P.: *Managing water resources: Methods and tools for a systems approach.*
1004 London: Earthscan James & James, 2009.

1005 Simonovic, S. P.: World water dynamics: Global modeling of water resources, *J. Environ.*
1006 *Manage.*, 66, 249-267, <https://doi.org/10.1006/jema.2002.0585>, 2002a.

1007 Simonovic, S. P., and Breach, P. A.: The role of water supply development in the Earth system,
1008 *Water*, 12, 3349, <https://doi.org/10.3390/w12123349>, 2020.

1009 Song, Q.: *Study on the wind resource distribution and wind power planning in China*, North
1010 China Electric Power University, 2013, (in Chinese).

1011 State Grid Energy Research Institution (SGERI), and China Nuclear Power Development
1012 Center (CNPDC): *Research on nuclear power development planning in China*. China Atomic
1013 Energy Press, 2019, (in Chinese).

1014 Stehfest E., van Vuuren D., Kram T., and Bouwman L.: *Integrated assessment of global*
1015 *environmental change with IMAGE 3.0: Model description and policy applications*, PBL
1016 Netherlands Environmental Assessment Agency, ISBN: 978-94-91506-71-0, 2014.

1017 Sterman, J. D.: *Business dynamics: Systems thinking and modeling for a complex world.*
1018 Boston: Irwin McGraw-Hill, 2000.

1019 Su, B., Huang, J., Zeng, X., Gao, C., and Jiang, T.: Impacts of climate change on streamflow
1020 in the upper Yangtze River basin, *Climatic change*, 141, 533-546,
1021 <https://doi.org/10.1007/s10584-016-1852-5>, 2017.

1022 Su, M.: Research on the coordinated development of energy in the Yangtze River Economic
1023 Zone, *Macroeconomic Management*, 12, 37-41, 2019 (in Chinese).

1024 Su, Y., Tesfazion, P., and Zhao, Z.: Where are the migrants from? Inter- vs. intra-provincial
1025 rural-urban migration in China, *China Economic Review*, 47, 142-155,
1026 [10.1016/j.chieco.2017.09.004](https://doi.org/10.1016/j.chieco.2017.09.004), 2018.

1027 Sullivan, P., Krey, V., and Riahi, K.: Impacts of considering electric sector variability and
1028 reliability in the MESSAGE model, *Energy Strateg. Rev.*, 1, 157-163,
1029 <https://doi.org/10.1016/j.esr.2013.01.001>, 2013.

1030 van Vuuren, D. P., Kok, M., Lucas, P. L., Prins, A. G., Alkemade, R., van den Berg, M.,
1031 Bouwman, L., van der Esch, S., Jeuken, M., Kram, T., and Stehfest, E.: Pathways to
1032 achieve a set of ambitious global sustainability objectives by 2050: Explorations using the
1033 IMAGE integrated assessment model, *Technol. Forecast. Soc.*, 98, 303-323,
1034 <https://doi.org/10.1016/j.techfore.2015.03.005>, 2015.

1035 Wang, H: Yangtze Yearbook, Changjiang Water Resources Commission of Ministry of Water
1036 Resources, 2015, (in Chinese).

1037 Wang, H., Liu, L., Yang, F., and Ma, J.: System dynamics modeling of China's grain
1038 forecasting and policy simulation, *Journal of System Simulation*, 21, 3079-3083, 2009. (in
1039 Chinese)

1040 Wang, Z., Nguyen, T., and Westerhoff, P.: Food-energy-water analysis at spatial scales for
1041 districts in the Yangtze river basin (China), *Environ. Eng. Sci.*, 36, 789-797,
1042 <https://doi.org/10.1089/ees.2018.0456>, 2019.

1043 Xie, H., and Wang, B.: An empirical analysis of the impact of agricultural product price
1044 fluctuations on China's grain yield, *Sustainability*, 9, 906,
1045 <https://doi.org/10.3390/su9060906>, 2017.

1046 Xu, X., Yang, G., Tan, Y., Liu, J., and Hu, H.: Ecosystem services trade-offs and determinants
1047 in China's Yangtze River Economic Belt from 2000 to 2015, *Sci. Total Environ.*, 634,
1048 1601-1614, <https://doi.org/10.1016/j.scitotenv.2018.04.046>, 2018.

1049 Yao, G., Gao, Z., and Li, X.: Evaluation of coal resources bearing capacity in China, *China*
1050 *Mining Magazine*, 29, 1-7, 2020 (in Chinese).

1051 Yangtze River Water Resources Commission (YRWRC): Water resources bulletin of the
1052 Yangtze river basin and the southwest rivers in China 2015. Yangtze River Press, Wuhan,
1053 2016 (in Chinese).

1054 Ye, L., Wei, X., Li, Z., et al.: Climate change impact on China food security in 2050, *Agron.*
1055 *Sustain. Dev.*, 33, 363-374, <https://doi.org/10.1007/s13593-012-0102-0>, 2013.

1056 Yi, B. L., Yu, Z. T., and Liang, Z. S.: Gezhouba Water Control Project and four famous fishes
1057 in the Yangtze River, Wuhan: Hubei Science and Technology Press, 1988, (in Chinese
1058 with English abstract).

1059 Yu, S., Yarlagadda, B., Siegel, J. E., Zhou, S., and Kim, S.: The role of nuclear in China's
1060 energy future: Insights from integrated assessment, *Energ. Policy*, 139, 111344,
1061 <https://doi.org/10.1016/j.enpol.2020.111344>, 2020.

1062 Yu, Z., Gu, H., Wang, J., Xia, J., and Lu, B.: Effect of projected climate change on the
1063 hydrological regime of the Yangtze River Basin, China, *Stoch. Env. Res. Risk A.*, 32, 1-
1064 16, <https://doi.org/10.1007/s00477-017-1391-2>, 2018.

1065 Zeng, Y., and Hesketh, T.: The effects of China's universal two-child policy, *The Lancet*, 388,
1066 1930-1938, [https://doi.org/10.1016/S0140-6736\(16\)31405-2](https://doi.org/10.1016/S0140-6736(16)31405-2), 2016.

1067 Zhang, C., Zhong, L., Fu, X., Wang, J., and Wu, Z.: Revealing water stress by the thermal
1068 power industry in China based on a high spatial resolution water withdrawal and
1069 consumption inventory, *Environ. Sci. Technol.*, 50, 1642-1652,
1070 <https://doi.org/10.1021/acs.est.5b05374>, 2016.

1071 Zhang, H., Kang, M., Shen, L., Wu, J., Li, J., Du, H., Wang, C., Yang, H., Zhou, Q., Liu, Z.,
1072 and Gorfine, H.: Rapid change in Yangtze fisheries and its implications for global
1073 freshwater ecosystem management, *Fish Fish.*, 21, 601-620,
1074 <https://doi.org/10.1111/faf.12449>, 2020.

1075 Zhang, H., Li, J. Y., Wu, J. M., Wang, C. Y., Du, H., Wei, Q. W., and Kang, M.: Ecological
1076 effects of the first dam on Yangtze main stream and future conservation recommendations:
1077 A review of the past 60 years, *Appl. Ecol. Env. Res.*, 15, 2081-2097,
1078 https://doi.org/10.15666/aeer/1504_20812097, 2017.

1079 Zhao, F., and Fan, Z.: The inhibitory effect of high housing prices on population inflows in the
1080 megacities: Based on the empirical evidence from the four cities of Beijing, Shanghai,
1081 Guangzhou and Shenzhen, *Urban Studies*, 26(03), 41-48, 2019. (in Chinese)

1082 Zhu, R., Ma, S., Yang, Z., et al.: Atlas of solar energy resources by province in China. Beijing:
1083 China Meteorological Administration, 2006, (in Chinese).